MISS DANILA CABRAL (Orcid ID : 0000-0003-1823-9135)

DR MOHAMED YOUSSEF BANORA (Orcid ID : 0000-0002-1663-525X)

DR JOSE DIJAIR ANTONINO (Orcid ID : 0000-0002-4992-0698)

DR LIEVEN DE VEYLDER (Orcid ID : 0000-0003-1150-4426)

DR JANICE DE ALMEIDA ENGLER (Orcid ID : 0000-0002-8312-672X)

Article type : Regular Manuscript

The plant WEE1 kinase is involved in checkpoint control activation in nematode induced galls

Danila Cabral[1], Mohamed Youssef Banora[1,2], José Dijair Antonino[1,3,4], Natalia Rodiuc[1,3], Paulo Vieira[1], Roberta R. Coelho[1,3], Christian Chevalier[5], Thomas Eekhout[6,7], Gilbert Engler[1], Lieven De Veylder[6,7], Maria Fatima Grossi-de-Sa[3] and Janice de Almeida Engler[1†]

[1]*INRA, Université Côte d'Azur, CNRS, ISA, 06903, Sophia Antipolis, France*

[2]*Department of Plant Pathology, Faculty of Agriculture, Ain Shams University, P.O. Box 68, Hadayek Shoubra, 11241, Cairo, Egypt*

[3]*Laboratório de Interação Molecular Planta-Praga, Embrapa Recursos Genéticos e Biotecnologia, PqEB, Av. W5 Norte final, Brasília, DF, 70770-900, Brazil.*

[4]*Departamento de Agronomia/Entomologia, Universidade Federal Rural de Pernambuco, Av. Dom Manoel de Medeiros S/N, Dois Irmãos, Recife, PE, 521171-900, Brazil*

[5]*UMR1332 BFP, INRA, University of Bordeaux, 33882 Villenave d'Ornon Cedex, France*

[6]*Department of Plant Biotechnology and Genetics, Ghent University, 9052 Ghent, Belgium*

[7]*VIB Center for Plant Systems Biology, 9052 Ghent, Belgium*

This article has been accepted for publication and undergone full peer review but has not been through the copyediting, typesetting, pagination and proofreading process, which may lead to differences between this version and the Version of Record. Please cite this article as doi: 10.1111/nph.16185

†Corresponding author: E-mail: janice.de-almeida@inra.fr; tel: +33492386459

ORCID IDs: 0000-0003-1823-9135 (DC), 0000-0002-1663-525X (MYB), 0000-0002-4992-0698 (JDA), 0000-0001-5627-2628 (PV), 0000-0002-5727-6206 (CC), 0000-0002-2878-1553 (TE), 0000-0003-1150-4426 (LDV), 0000-0001-8184-9599 (MFGS), 0000-0002-8312-672X (JAE)

Received: 12 April 2019
Accepted: 15 August 2019

Summary

• Galls induced by plant-parasitic nematodes involve a hyperactivation of the plant mitotic and endocycle machinery for their profit. Dedifferentiation of host root cells includes drastic cellular and molecular readjustments. In such background, potential DNA damage in the genome of gall cells is eminent.

• We questioned if DNA damage checkpoints activation followed by DNA repair occurred, or was eventually circumvented, in nematode-induced galls.

• Galls display transcriptional activation of the DNA damage checkpoint kinase WEE1, correlated with its protein localization in the nuclei. The promoter of the stress marker gene SMR7 was evaluated under the WEE1-knockout background. Drugs inducing DNA damage and a marker for DNA repair, PARP1 were used to understand mechanisms that might cope with DNA damage in galls.

• Our functional study revealed that gall cells lacking WEE1 conceivably entered mitosis prematurely disturbing the cell cycle despite the loss of genome integrity. The disrupted nuclei phenotype in giant cells hinted to the accumulation of mitotic defects. As well, WEE1-knockout in Arabidopsis and downregulation in tomato repressed infection and reproduction of root-knot nematodes. Together with data on DNA damaging drugs, we suggest a conserved function for WEE1 controlling a G1/S cell cycle arrest in response to replication defect in galls.

Keywords: *Arabidopsis thaliana*, cell cycle, checkpoint control, galls, root-knot nematode, *Solanum lycopersicum*, WEE1 kinase

Words count total:
Main body: 6790

Introduction: 871
Material and methods: 1279
Results: 2008
Discussion: 2636
Concluding remarks: 243
Acknowledgements: 73
Author Contributions: 48
References: 2171
Figure legends: 1731
Figures: 14 Figures. Colored Figures: 1, 2, 3, 6, 7, 8, 10, 11 & 14
Supporting information: 5 Figures & 6 Movies

Introduction

The integrity of the plant genome is continuously threatened by external stresses such as pathogen attack capable to induce replication errors leading to DNA damage. Plant-parasitic root-knot nematodes (RKN; Meloidogyne spp.) are economically devastating endoparasites (Shukla *et al.*, 2017) that disturb the plant cell cycle, triggering hyperproliferation and tumorigenesis creating feeding sites, named galls (de Almeida Engler *et al.*, 1999, 2012, 2015). These nematode-induced feeding sites (NFS) enclose around 7 giant-feeding cells (GCs) surrounded by asymmetrically dividing neighboring cells (NCs). Their development is characterized by a mitotic phase illustrating defective spindles and absence or aborted phragmoplast in GCs with aborted cytokinesis, followed by an endocycle phase resulting in enlarged highly invaginated nuclei (de Almeida Engler *et al*., 2004; Antonino de Souza Junior *et al*., 2017). Early host cell cycle hyperactivation in NFS is distinguished by the expression of core cell cycle genes like CDKs and CYCs (de Almeida Engler *et al.*, 1999). As well, inhibitors as KRPs and DEL1 play a part restraining the cell cycle most likely to regulate gall growth and development to an assured level (de Almeida Engler *et al.*, 2012; Vieira *et al.*, 2012, 2013, 2014). Likewise, the switch from mitotic to endoreduplication cycles was shown to involve *CCS52* genes during gall expansion (de Almeida Engler *et al.* 2012). Alongside, all data evidence the compelling involvement of the cell cycle for gall genesis and development. Seen the cell cycle hyperactivation, it is to be expected that gall development might not only account for mitotic defects, but as well for the induction of DNA damage and loss of genome integrity. Upon DNA

damage plant or animal cells activate checkpoint control pathways (Hu *et al.*, 2016). These pathways introduce a delay in cell cycle progression while DNA repair enzymes restore DNA anomalies, including base pair mismatches, abnormal bases, stalled replication forks, single-stranded DNA breaks (SSBs), and double-stranded DNA breaks (DSBs) (Friedberg *et al.*, 2006). Thus, the cells have enough time to repair its damaged DNA before advancing to the next cell cycle phase. Previous reports have shown that bacteria, fungi and oomycetes pathogens induce double strand breaks (DSBs) in host plants (Song and Bent, 2014). Alternatively, microbes contribute to tumorigenesis by directly inducing DNA damage, potentially inactivating checkpoint controls, or manipulating repair processes (Weitzman & Weitzman, 2014).

One particular gene involved in DNA damage checkpoint control is *WEE1*, encoding for a protein kinase that was first described in fission yeast as a rate-restriction step for the G2-to-M transition through the inhibition of activity of cell cycle rate-limiting factors, cyclin-dependent kinases (CDKs) (Russell and Nurse, 1987; De Schutter *et al.,* 2007**)**. The Arabidopsis *WEE1* kinase gene appears to be non-essential for plant growth but is essential when plants experience problems during the replication phase, such as induced by the replication blocking agent hydroxyurea (HU). Whereas wild-type plants delay their S phase in the presence of HU, WEE1 deficient plants fail to do so, eventually resulting in a permanent cell cycle arrest, likely due to accumulation of replication defects (Cools *et al.*, 2011). Within the root meristem, *WEE1* transcript levels cannot be detected in the absence of DNA damage, but its expression is quickly and strongly induced upon DNA stress in an ATM (ataxia telangiectasia mutated) or ATR (ATM and Rad3-related) dependent manner (De Schutter *et al.*, 2007). ATM and ATR are main regulators of the DNA damage response (DDR) and both sense DNA damage and induce the coordinated expression of DNA repair and cell cycle arresting genes. ATM is recruited and activated in reply to ionizing radiation, radiomimetic agents, and agents which trigger double-strand DNA breaks (Garcia *et al.*, 2003). Conversely, *ATR* is activated by a broader range of genotoxic stimuli resulting in single-strand DNA breaks and stalled replication forks (Culligan *et al.*, 2004). The plant-specific transcription factor SOG1 is also a central regulator of the DDR pathway and its activation is required for responses to DNA damage, including transcriptional responses, cell-cycle arrest and death of stem cells (Yoshiyama *et al*., 2013).

Herein we highlight that the hyperactivation of the cell cycle used to generate a nematode-induced gall in plant host roots might cause eminent DNA damage in the genome. If yes, during stress caused by nematode infection we question if host cells will arrest or induce the cell cycle, or else if the endocycle is activated or cell death is induced. Instead, nematodes might inhibit checkpoint activation

for a successful interaction as seen reported for other microbes (Song and Bent, 2014; Weitzman & Weitzman, 2014).Along these lines, this topic was never addressed before during plant-nematode interactions and very few data is found in the literature for other plant pathogens. We demonstrate that the Arabidopsis *WEE1* gene is transcribed in response to nematode attack, suggesting that infection goes along with DNA damage checkpoint activation in NFS. Functional analysis and treatments that induce either DNA damage or DNA replication stress suggested the timely involvement of WEE1 kinase on cell cycle arrest. As well, WEE1-knockout in Arabidopsis and downregulation in tomato resulted in less developed galls consequently repressing infection and reproduction by root-knot nematodes. Furthermore, drugs inducing DNA damage and a marker for DNA repair, *PARP1*, were employed here to understand mechanisms that might cope with DNA damage in Arabidopsis galls.

Material and Methods

Arabidopsis *in vitro* growth conditions and nematode infections

Approximately 50 seeds of *Arabidopsis thaliana* Col-0 (hereafter referred as wild-type) and *WEE1* knockout line (*wee1-1*; De Schutter *et al.,* 2007) were surface-sterilized (Vieira *et al*., 2013). Seeds were germinated in MS medium, and for the *wee1-1* line containing 50mg/L sulfadiazine. Seedlings were grown vertically allowing roots to stay at the surface under a 16/8 h (light/dark) photoperiod at 21°C/18°C. Each seedling was then infected with 100 surface-sterilized (Coelho *et al.,* 2017) and freshly hatched *Meloidogyne incognita* juveniles and galls of infected roots were harvested for several tests as described below.

Tomato growth conditions and infection

Cherry tomato (*Solanum lycopersicum* Mill. cv West Virginia106-Wva106) wild-type plants, two *WEE1* antisense lines (*WEE1*^{AS}): *Wee1* L8.3 AS and *Wee1* L73.10 AS(*Pro35S:Slwee1AS*), transgenic lines (Gonzalez *et al.,* 2007; Mathieu-Rivet *et al*., 2010) were grown in a growth chamber under a thermoperiod of 25°C/20°C and a photoperiod of 14/10 h (light/dark). For nematodes inoculation, around 1000 freshly hatched second stage juveniles (J2s) of *Meloidogyne incognita* were inoculated for each 14 day-old seedlings. Infected tomato seedlings were kept at 25°C with a 16-h photoperiod for 40 days to allow nematodes to complete their life cycle. At 40 days after inoculation (DAI), galls and egg mass numbers were counted and scored.

Histochemical GUS analyses of Arabidopsis galls

Plants harboring *WEE1:GUS*, *SMR7:GUS,* and *PARP1:GUS* in wild-type (Col-0) or in the *wee-1* background were nematode infected and galls were collected at different time points after inoculation (3, 5, 7, 14, 21, 30 DAI). The *wee1-1* and *SMR7:GUS* lines have been previously described by De Schutter *et al.,* (2007) and Yi *et al.* (2014)respectively. To generate the *SMR7:GUS* line in *wee1-1* background, *wee1-1* and *SMR7:GUS* lines were crossed and selected on both kanamycin (35 µg/ml) and sulfadiazine (7.5 µg/ml). GUS assays were performed according to de Almeida Engler *et al.,* (1999). Galls were harvested and embedded in Technovit 7100 (Heraeus Kulzer) as described by the manufacturer, sectioned (3 µm) and analyzed by dark-field microscopy optics by an Axiocam camera (Zeiss).

mRNA *in situ* hybridization assays on Arabidopsis galls

Dissected galls of Arabidopsis wild-type (Col-0) at 7, 14 and 30 DAI were collected, fixed in 2% glutaraldehyde, paraffin embedded and sectioned (10µm). All *in situ* hybridization steps have been performed essentially as described by de Almeida Engler *et al*., (2009). Gene specific sense and antisense probes of *WEE1* were generated and hybridized with gall sections. Sections were developed, stained with 0.05% toluidine blue and analyzed by dark-field optics.

Morphological analysis, nuclei staining and giant cells measurements in Arabidopsis and tomato galls

For morphological observation *Arabidopsis thaliana wee1-1* and wild-type (Col-0) and *Solanum lycopersicum WEE1^{AS},* and wild-type (SR1) uninfected roots and galls were collected. For Arabidopsis, galls of *wee1-1* (1, 3, 5, 7, 14 and 21 DAI) and wild-type (3, 7, 14 and 21 DAI) were dissected at different time points. In transgenic tomatoes, morphological analysis was performed in the two *WEE1* antisense lines: *Wee1* L8.3 AS and *Wee1* L73.10 AS, and the wild-type line as a control at 7, 14 and 30 DAI. Having in the *WEE1* antisense lines similar gall phenotypes we then further focused on the *Wee1* L73.10 AS (named *WEE1^{AS}*). Galls of *wee1-1, WEE1^{AS}* treated as described by de Almeida Engler *et al.,* (2012) and then embedded in Technovit 7100 (Heraeus Kulzer) as described by the manufacturer. Embedded gall tissues were sectioned (3 µm), stained in 0.05% toluidine blue and imaged with a digital camera (Axiocam, Zeiss).

For nuclei observations sections of all transgenic lines (*wee1-1, WEE1^{AS}*) and wild-type controls studied here, and Arabidopsis treated with DNA damage inducing drugs (bleomycin or hydroxyurea) were stained

with 1µg/mL 4',6-diamidino-2-phenylindole (DAPI). Slides were analyzed by epifluorescence microscopy. Giant cells measurements were performed in two of the biggest GCs per gall using the Axioplan software (Zeiss). A minimum of 30 GCs were recorded per line and evaluated by analysis of variance, using the SPSS software (version 10, Chicago, IL).

Morphological analysis and volume measurements of giant cells nuclei

For nuclear structure and morphology observation thick gall slices were cleared and stained with 6-diamidino-2-phenylindole (DAPI) essentially as described by Antonino de Souza Junior *et al.,* (2017). Galls were mounted in 90% glycerol and imaged using a Zeiss LSM 880 confocal microscope. Dye excitation was performed with a diode 405nm laser and fluorescence was gathered between 431 and 532 nm. Z-stacks were generated from approximately 60 images with a 1 µm optical slice thickness and used to generate maximum brightness projections. For volumetric measurements of GC individual nuclei of wild-type and *wee1-1* from image stacks of DAPI-stained galls were analyzed with the plugin Volumest (http://lepo.it.da.ut.ee/~markkom/volumest/) from the public domain ImageJ software. Analysis was performed precisely as described by Antonino de Souza Junior, *et al.* (2017).

***In vivo* localization of GFP-WEE1 in Arabidopsis galls**

In vivo observations of nematode infected roots of the *35S:GFP-WEE1* line was performed by confocal microscopy (Zeiss LSM 510 META). Galls at different time points after inoculation (3, 6 and 7 DAI) were analyzed. Dye excitation was carried out with a 543nm HeNe laser and emission light was captured with a long pass 560 emission filter. Z-stacks were produced using 1 µm thick optical sections and images are represented as maximum brightness projections.

Flow cytometry analyses of Arabidopsis and tomato galls

Transgenic and wild-type Arabidopsis (*wee1-1* and wild-type) and tomato (*WEE1*^{AS} and wild-type) uninfected roots and galls were analyzed for their ploidy levels by flow cytometry. Galls and roots 21 DAI were harvested in water and immediately prepared for flow cytometry precisely as described by Vieira *et al*., (2013). Nuclei were then stained with 20µg/mL propidium iodide (Sigma). After samples were examined the mean values of repetitions of independent experiments were calculated, and the fraction of nuclei with ploidy levels from 2C to 64C for Arabidopsis and 2C to 128C for tomato was expressed as the percentage of the total number of nuclei measured.

Bleomycin and hydroxyurea treatments on Arabidopsis galls

To test whether WEE1 plays a role in the G1/S or G2/M checkpoints, drug treatment inducing DNA damage, hydroxyurea and bleomycin were performed, and compared to non-treated nematode infected seedlings. Thus, wild-type *wee-1-1* were germinated on MS medium and transferred 7 DAI to the same medium supplemented with 5 mM hydroxyurea (HU) or 0,3 µg/mL bleomycin (BL) and incubated 14 days at room temperature. As controls, nematodes were incubated with similar concentrations of HU and BL and tested for infectivity as described by de Almeida Engler *et al*., (1999, 2004). Control experiments were performed using the same medium in the absence of inhibitors. Morphological analysis was performed as described above and subsequent sections were stained with 6-diamidino-2-phenylindole (DAPI) for nuclear observation. To test if the promoter of the DNA repair gene *PARP1* and the stress marker *SMR7:GUS* and *SMR7:GUS* in *wee1-1* were induced in developing galls (7, 14 and 21 DAI) *M. incognita* infected roots GUS lines were treated with 5mM HU and 0.3 µg/mL BL for 24 h.

Nematode infection tests on Arabidopsis

Arabidopsis seedlings were germinated and grown in soil precisely as described by de Almeida Engler *et al*. (2016). Three-week-old wild-type (Col-0) seedlings and *wee1-1*were inoculated each with approximately 200 stage 2 juveniles (J2) of *M. incognita*. Data shown for each line represent means ± SD of 20 seedlings analyzed during two independent biological repetitions. Six weeks after inoculation the numbers of galls and egg masses per plant were recorded.

Statistical Analysis

All quantitative data of Arabidopsis and tomato such as galls and egg mass number, giant cell area and nuclei volume were statistically analyzed by Analysis of Variance (ANOVA) and Tukey´s test, or Student's t-test (the significance level was set at 0.05).

Results

***WEE1* promoter activity and transcript accumulation were detected in young galls of Arabidopsis**

The analysis of promoter activity and transcript localization of *WEE1* are shown in Figure 1. Promoter activity of *WEE1* was not observed in uninfected root but was already observed in foring GCs (3 DAI) and became stronger during the mitotic phase of gall development (5-7 DAI). *WEE1* expression was detected in GCs as well as in NCs, but was weaker and patchy at 14 DAI and nearly absent 21 and

30 DAI (Fig. 1a). To determine if promoter activity reflected accurately the endogenous transcript localization, *in situ* mRNA localization was performed in gall sections using a *WEE1* antisense probe (Fig. 1b). *WEE1* transcripts were present in GCs as well as in NCs at 7 DAI, decreased at 14 DAI and expression was virtually absent in mature galls 21 DAI, but still present in proliferating gall xylem. Control hybridization with the sense probe gave no hybridization signal. Accordingly, the *in situ* transcript localization observed (Fig. 1b) was consistent with the promoter activity assessed by GUS assays (Fig. 1a).

WEE1 was nuclear localized *in vivo* in Arabidopsis galls

Using a translational fusion between GFP and WEE1 (GFP-*WEE1)* under control of the *WEE1* promoter, the subcellular localization of WEE1 was studied in nematode infected root cells of Arabidopsis, showing its exclusive localization in the plant cell nucleus (Fig. 2). WEE1 was observed very early (3 DAI), and was essentially present in the feeding sites compared to other root sites (Fig. 2a, b). A patchy pattern of GFP-fluorescent nuclei was seen, suggesting that not all gall cells expressed *WEE1* (Fig. 2**c**). Young galls (6 and 7 DAI) showed strong nuclear fluorescence of the GFP-WEE1 fusion protein (Fig. 2c and d) corroborating with results on promoter activity and mRNA *in situ* localization.

The lack of WEE1 in Arabidopsis leaded to increased mitotic activity in galls

Evaluation of RKN-induced gall development in the absence of WEE1 showed that nematodes can infect the *wee1-1* mutant line and induce a feeding site (Fig. 3a). In *wee1-1* galls, high mitotic activity was observed as evidenced by the apparent increased nuclei number in GC and ectopic proliferation of NCs (Fig. 3a). Often larger vacuoles and cell wall stubs (obvious in gall images of 7 and 14 DAI; Fig. 3a) were visible in developing GCs. These cell wall fragments illustrate that despite the replication problems mitotic activity continues in GCs resulting in aberrant mitosis. Disordered and asymmetrically dividing cells surrounding young GCs (3 and 5 DAI) were more evident in the *wee1-1* mutant line, compared to the wild-type (Fig. 3b), and feeding cells were apparently smaller indicating a hindrance in gall development (Fig. 3a). Cell walls in GCs presented invaginations and regions showing thinner cells walls indicating the presence of plasmodesmata (14 DAI, Fig. 3a) as normally seen in wild-type galls (Rodiuc *et al.*, 2014). In mature galls (21 DAI) layers of elongated cells morphologically like xylem cells and xylem vessels were evident surrounding GCs.

WEE1 knockout induced an altered nuclear morphology and volume in giant cells

To verify if *WEE1* knockout affected nuclear morphology in GCs, DAPI stained thick gall sections were visualized by confocal microscopy to have a three-dimensional (3D) microscopic view. During mitotic divisions in GCs (7 DAI) of *wee1-1* small elongated nuclei could be seen, and this phenotype became more evident in maturing galls (14 DAI) when nuclei were elongated and apparently interconnected (Fig. 4a). Although convoluted, nuclei shape in wild-type GCs was almost always amoeboid like (Fig. 4b) and not elongated as seen in *wee1-1* (Fig. 4a). Not surprisingly, volumetric measurements at 14 DAI revealed larger nuclei volumes in GCs of the *wee1-1* line compared to the wild-type (Fig. 4c). This result, together with observed cell division phenotypes, suggests that cumulative mitotic defects might have occurred in *wee1-1*galls upon the impairment of checkpoint activation.

Flow cytometric analysis revealed mitotic stimulation in galls

Nuclear ploidy levels of *wee1-1* control wild-type galls (21 DAI) and gall-less roots were measured by flow cytometry (Fig. 5). Analyses revealed that the DNA ploidy levels in roots of *wee1-1* decreased compared to wild-type. In roots the 2C ploidy level increased in the *wee1-1* mutant line increased but the 4C to 16C levels slightly decreased compared to the wild-type (Fig. 5a**;** S1a). In *wee1-1* galls, 2C DNA content increased most likely derived from the ectopic NC division (Fig. 5b; S5b) and decreased ploidy levels were seen at 4C to 16C. Subtle increase in 32C and 64C in GCs might be derived from the elongated nuclei in the *wee1-1 line.*

***SMR7:GUS* activity was high upon WEE1 knockout**

The siamese-related cyclin-dependent kinase inhibitor gene *SMR7* reacts strongly to genotoxic stress response in a likely ROS-dependent manner (Yi *et al.*, 2014). To find out if *SMR7* promoter was activated in galls in response to stress, we performed GUS assay using the line harboring the *SMR7:GUS* transcriptional reporter construct in the *wee1-1* background (no checkpoint control activation) and in the wild-type during gall development (7, 14 and 21 DAI) (Fig. 6). These tests revealed a strong induction of the *SMR7* promoter in galls in the transgenic line under the *wee1-1* background compared to the wild-type (Fig. 6a). In contrast, in the wild-type background a weak *SMR7* promoter activity was seen in young mitotic galls (7 DAI), in maturing endoreduplicating GCs (14 DAI), ultimately disappearing overall in full-grown feeding sites undergoing the lowest cell cycle activity (21 DAI) (Fig. 6b).

Effect of DNA damage caused by drugs in *wee1-1* galls and wild-type

In order to interfere with the cell cycle checkpoint (G2/M and G1/S), we introduced two drugs in media containing infected plants and observed *WEE1:GUS* activity, gall morphology, nuclei distribution, GCs area and ultimately performed infection tests. To induce the replication arrest checkpoint at G1/S phase of the cell cycle hydroxyurea (HU) was used as an inhibitor of the ribonucleotide reductase, in this way inhibiting DNA replication. Previous work has shown that plants treated with HU show reduced deoxynucleotide triphosphate (dNTP) levels, as a result affecting replication fork progression causing replication stress (Wang & Liu, 2006; Saban & Bujak, 2009). To activate checkpoint control at G2 phase we used the drug bleomycin (BL), inducing DSBs in plant cell DNA. Bleomycin acts by inhibiting the incorporation of thymidine into DNA strands producing reactive oxygen species that directly damage the DNA and RNA causing DNA cleavage (Takimoto & Calvo, 2008). Both BL and HU have been used at a dose that had mild, but perceptible, effects on gall development. As well, pre-treatments of juvenile nematodes with drugs compared to non-treated showed that they infected Arabidopsis roots normally. Thus, upon drug treatments nematodes did not lose their infectivity competence seemly due to their strong cuticle (de Almeida Engler *et al.*, 1999, 2004).

Effect of drug treatments on WEE1 promoter activity and on gall morphology

Expression patterns of *WEE1:GUS* NFS 10 DAI showed in non-treated galls a basal level of *WEE1* expression in all young GCs that significantly increased upon HU treatment (7, 14, 21 DAI in Fig. 7a and Fig. S2). However, this pattern was weak or patchy for GCs treated with BL (Fig. 7a). Morphological analysis of non-treated*WEE1*-deficient plants confirmed high mitotic activity in galls (Fig. 3a, 7b) which was visibly increased upon BL treatment showing ectopic proliferation of NCs (Fig. 7b, 8b) and enlarged GCs (Fig. 9a). Interestingly, HU treatment in the *wee1-1* line led to the appearance of cell wall stubs in GCs, and feeding-cells were larger than in wild-type galls (Fig. 7b). In wild-type, BL and HU treated galls displayed GCs containing numerous cell wall fragments with some GCs apparently dividing (Fig. 7c).

Nuclei structure in giant cells in the presence and absence of WEE1 and upon drug treatments

Galls from the same group of sections used for morphological analysis (Fig. S3**)** and thick gall sections were DAPI stained to visualize nuclei (Fig. **8**). Interestingly a fraction of non-treated *wee1-1* (-WEE1) galls presented visibly smaller nuclei and the other part were apparently connected and elongated, likely as a result of accumulation of mitotic errors (Fig**.** 4, 8a, Video S1). In contrast, larger nuclei and the increased mitotic activity in BL and HU treated galls was striking (Fig. 8b, c, Video S2,

S3). Wild-type (+WEE1) galls BL or HU treated also showed enlarged nuclei compared to the non-treated (Fig. 8 d, e, f, Videos S4, S5, S6) with seemly unstructured nuclei seen during BL treatments (Fig. 8e, Video S6). As well, reduced GC area for BL treatments was seen compared to non-treated (Fig. 9a). These phenotypes suggest a link to a premature mitotic entry of gall cells and the observed inhibition on gall induction and egg mass production by nematodes (Fig. 9b, c). As well, wild-type HU and BL treated galls will most likely trigger a delay in *WEE1* driven checkpoint activation (Cools *et al.*, 2011) resulting in GCs harboring cell wall stubs (Fig. 7c). These results suggest higher mitotic activity in GCs substantiating similarly seen in *wee1-1* galls.

Giant surface area was altered in WEE1-deficient galls and upon drug treatments

WEE1-deficient galls were more mitotic but showed decreased GC surface area (Fig**.** 9a). Curiously, as mentioned above BL and HU treatments of galls in the *WEE1*-defficient GCs showed a larger surface compared to non-treated (Fig. 9a). This possibly contributed with the intriguingly observed increased reproduction in drug treated WEE1-deficient galls (Fig. 9c). Moreover, more galls were induced in the *wee1-1* line BL or HU-treated (Fig. 9b).

PARP1pro:GUS activity was high in galls and in response to stress inducing drugs

To investigate if the DNA repair process or signaling pathways sensing alterations in genome integrity occurs in galls, the *PARP1* [poly(ADP-ribose) polymerase 2] gene promoter activity was analyzed. The *PARP1:GUS* reporter line was infected with nematodes and GUS assays revealed strong expression of *PARP1* in galls at different developmental time points (Fig. 10a). Promoter activity was high in GC and in NCs at 7 DAI. From 14 DAI until 21 DAI, the *PARP1:GUS* expression was variable among GCs and interestingly stronger close to the nematode head (Fig. 1 0a). Considering the strong expression of *PARP1:GUS* in galls during long incubations (16 h), we also performed shorter tests (3 h) (Fig. 10b) during drug-induced stress treatments to better perceive GUS expression. Non-treated galls under short incubations (3 h) showed weak *PARP1*expression, whereas *PARP1* promoter activity was slightly stronger upon BL treatment, but increased significantly upon HU treatment (Fig. 10b). These observations suggest that DNA damage might be followed by repair, but galls were more reactive to single-strands breaks.

The lack of _WEE1_ in tomato plants delayed gall development and decreased nematode reproduction

To evaluate the effect of *WEE1* downregulation in an important crop host we investigated its role during nematode infection in tomato plants of two lines expressing *WEE1*^{AS}. Galls of 7, 14 and 30 DAI from the transgenic line *WEE1*^{AS} were collected, analyzed for their morphology and compared to wild-type (Fig. 11 and Fig. S4). Although nematodes succeeded to infect roots of *WEE1*^{AS} transgenic lines, galls were apparently smaller and a delay or an arrest in nematode maturation was visible (Fig. 11a to be compared with Fig. 11b, c). To some extent more NC divisions were seen upon *WEE1* downregulation (Fig. 11b) compared to the wild-type (Fig. 11a) as observed in Arabidopsis galls (Fig. 3a). DAPI stained nuclei, of gall sections coming from the same batch used for morphological analysis, revealed that nuclei of *WEE1*^{AS} were apparently smaller than in wild-type mature galls (30 DAI), even when endoreduplication has taken place (Fig. 11). As well, a large number of intensely stained nuclei (7 and 14 DAI) was seen surrounding *WEE1*^{AS} GCs (Fig. 12b compared to Fig. 12a).

Giant cell and flow cytometry measurements and infection tests in tomato *WEE1*^{AS} line

Measurements in tomato GC showed that their surface was smaller upon *WEE1* downregulation compared to wild-type (Fig. 13a). This data can be correlated with the low reproduction ratios in both transgenic lines where small numbers of egg masses were recorded (Fig. 13b). Flow cytometry measurements revealed slightly decreased ploidy levels in the *WEE1*^{AS} line gall-less roots and galls as visualized during DAPI staining (Fig S5).

Discussion

In response to DNA damage, eukaryotic cells activate elaborate cellular networks, collectively termed, the DNA damage response (DDR). The DDR pathway senses DNA breaks arresting the cell cycle and repairing DNA lesions, being crucial for maintenance of the genomic integrity and plant survival. The Arabidopsis *WEE1* gene is activated by DNA damage or by DNA-replication arrest and is a downstream target gene of the ATR-ATM signaling cascades (de Schutter *et al.*, 2007; Cools *et al.,* 2011).WEE1 has been identified as an important target of the DNA replication (G1/S) and DNA damage (S/G2) checkpoints and is considered the main regulator of the S-phase checkpoint in plants (Cools *et al.,* 2011). So far, it is unknown if checkpoint control activation occurs in galls upon nematode infection. We show here that the Arabidopsis *WEE1* gene is transcriptionally activated and nuclear localized in galls as well in response to treatments that induce either DNA damage or DNA replication stress. We further demonstrate that *AtWEE1* knockout as well as *SlWEE1* (from tomato) knockdown inhibits gall development consequently significantly decreasing nematode reproduction.

WEE1 expression and protein localization suggest the activation of a checkpoint control in Arabidopsis galls

Based on results of *WEE1* promoter activity, mRNA and protein localization in galls we reasoned that the WEE1 kinase may be involved in checkpoint control induction throughout the gall including GCs and their neighboring cells (NCs) during the nematode infection process in host-plants. Early gall expression of *WEE1* suggests that DNA damage or a lag in completing DNA synthesis might be occurring. At this stage nuclei are intensely and synchronously dividing and often chromosome segregation during mitotic events often appears disturbed (de Almeida Engler *et al.*, 2004), therefore most likely more prone to DNA damage. Thus, during the mitotic phase of gall development potential damage during replication may occur especially in GCs activating checkpoint at G1/S, seen by the chronological *WEE1* expression. The replication checkpoint will relieve DNA replication stress by stabilizing replication forks, inhibiting origin firing and reducing the replication speed (Cools *et al.,* 2011). Herein, *WEE1* expression in gall nuclei might cause an accumulation of phosphorylated inactive CDKs slowing down mitosis and limiting excessive and uncontrolled mitotic activity. In addition, WEE1 accumulation in the polyploid GC nuclei could be related to DNA stress caused by the presence of the nematode. Studies of mechanisms leading to endoreduplication in human keratinocytes have shown that DNA damage may lead to polyploidy. Thus, a damage differentiation response (DDR) might to a certain level contribute to limit nuclei and cell proliferation in galls, subsequently causing a polyploidy rise in GCs. Indeed, it is believed that plants and animals profit of endoreduplication to enable tissue growth upon DNA damage (Adachi *et al.*, 2011).

The absence of WEE1 in galls provoke ectopic mitotic activity

Although plants lacking a functional WEE1 are indistinguishable from wild-type (De Schutter *et al.*, 2007), RKN-induced galls showed obvious mitotic division phenotypes. This was illustrated by the induced nuclei number, presence of wall stubs and occasional presence of complete cell walls in GCs suggestive of stimulated cytokinesis. Induced cell division was also evident in NCs and xylem tissue, suggesting that lack of WEE1 in galls brought cells into a resilient mitotic state. Consistently, *WEE1* expression has been observed in dividing tissues of Arabidopsis seedlings (De Schutter *et al.*, 2007) and in tobacco BY2 cells treated with dexamethasone (Siciliano *et al.*, 2019). The reduced GCs size and elongated and apparently

interconnected nuclear morphology in maturing GCs in the WEE1-deficient line indicated the inability to slow down or arrest mitosis. These perceived mitotic defects did not lead to cell death, as observed in root meristems (Cools *et al.*, 2011). Data on flow cytometry confirmed a shift of gall cells into a mitotic state, even when ploidy levels in GCs were not clearly changing most likely due to their disturbed nuclei phenotype. Anomalies in the detection of DNA damage upon *WEE1* deficiency, most likely prevented checkpoint control activation in galls which progressed into an unrestrained mitotic state leading to the elongated nuclear shape. As well, occurrence of cumulative ratios of replication errors in GC nuclei lacking *wee1* might inhibit DNA repair and cause replication stress as observed in cancer tissues (Halazonetis *et al.*, 2008; Zeman et al., 2014). Finally, a lack of checkpoint control activation in *wee1-1* galls allowed nuclei to further divide despite DNA damage, thus likely promoting genomic instability and delaying the endocycle. Thus, gall cells lacking WEE1 conceivably entered mitosis prematurely disturbing the cell cycle despite the loss of genome integrity. Furthermore, strong and long-term induction of the *SMR7* promoter in the absence of WEE1, suggests that WEE1 induces checkpoint control in order to avoid catastrophic defects during the hyperactivation of the mitotic and endocycle in GCs. The lack of WEE1 might result in continued division in the presence of replication damage, which eventually might cause DSBs and hence induction of *SMR7*. Three *SIAMESE/SIAMESE-RELATED* (*SIM/SMR*) cyclin-dependent kinase inhibitors were reported strongly reacting to genotoxicity, of which *SMR5* and *SMR7* were confirmed to be checkpoint regulators (Yoshiyama *et al.*, 2013; Yi *et al.*, 2014). These *SMR*s are strongly induced by treatment of DSBs inducing agents and are identified as part of a signaling cascade inducing cell cycle checkpoint in response to ROS-induced DNA damage (Wei *et al.*, 1998; Morin et al, 2011; Yi *et al.*, 2014). In addition, upregulation of the *SMR7* promoter suggests genotoxicity stress upon nematode infection. -

WEE1-deficient galls show hypersensitivity to DNA replication stress caused by hydroxyurea

Although WEE1-deficient plants present normal development, they are hypersensitive to DNA-damage caused by HU (De Schutter *et al.*, 2007). Therefore, treatments of nematode-infected roots impeding DNA replication (HU) or causing DNA double strand breaks (BL) on the wild-type (+WEE1) and in WEE1-deficient line (-WEE1) helped us to understand the relevance of the WEE1 kinase in galls. The *WEE1* expression in galls strongly responded to inhibition of replication forks caused by HU and less to double strand DNA breaks caused by BL. In fact, HU treatment mimics what happens in WEE1-deficient line causing replication defects accounting for the observed gall phenotype. Galls silenced for the replication stress checkpoint activators *WEE1* are HU hypersensitive indicating that HU-

induced replication stress prevails in galls as occurring in uninfected roots (De Schutter *et al.*, 2007). These results suggest that the WEE1-induced checkpoint control activation in galls seems more associated to the G1/S phase. Moreover, a remarkable enhanced mitotic activity in galls (more nuclei in GCs and more NCs) in the *wee1-1* mutant line under stress conditions caused by BL and HU treatment was perceived. Interestingly enhanced susceptibility was observed in galls induced in the *wee1-1* line treated with BL or HU when checkpoint control is not active but repair normally is not inhibited (Cools *et al.*, 2011). This data suggests that even when DNA is damaged in gall cells, with no checkpoint activation (-WEE1), GCs can develop suggesting that nematodes profit of this status to efficiently induce feeding sites. Thus, besides that NFS might have unique mechanisms adapting their growth strategy a lack of regulation of the cell cycle upon WEE1-knockout might affect the host immune system leading to high vulnerability of nematode attack. The increased GC surface seen in WEE1-deficient galls treated with HU possibly contributed with this enhanced susceptibility observed by the increased gall and egg mass numbers. As well, although the *wee1-1* line is sensitive to replication inhibiting chemicals, the mitotic index in the root meristem does not decrease upon HU treatment (De Schutter *et al.*, 2007). Interestingly Cools *et al.* (2011) reported that *wee1-1* and wild-type plants behave similarly in the absence of DNA damage stress, but upon HU treatment 251 genes were differentially regulated. The absence of a functional *WEE1* in Arabidopsis showed a significant induction of distinct histone genes which in this context could facilitate cell cycle progression during gall development seen during our HU treatment. During HU treatment, high *WEE1* expression in galls is most likely associated with replication stress in an ATR-dependent manner. Thus, WEE1-deficient galls may fail to activate a checkpoint control arrest and progress through the cell cycle with a not fully replicated genome into mitosis. As well, no checkpoint control activation added to the BL induced DSBs enhanced mitotic activity, most likely contributed to the observed increased nematode reproduction. In contrast, gall induction and reproduction (egg mass number) in the wild-type was low during both treatments suggesting the checkpoint activation by HU during G1/S or by BL during G2/M phases. This would delay the cell cycle to gain time for repairing the DNA damage in galls. As for galls, root meristems are sensitive to replication-inhibiting chemicals, showing a clear growth inhibition phenotype. *WEE1* transcript levels are high after HU treatment showing that replication inhibition may activate the *WEE1* gene in galls as for non-infected seedlings (De Schutter *et al.*, 2007). During bleomycin treatment on wild type galls the WEE1 protein will possibly prevent nuclei to enter mitosis via the inhibition of complexes involved in the G2-to-M transition. Upon the incidence of

DNA stress caused by HU or BL, *WEE1* expression might be maintained, arresting cells in the G1-phase or G2-phase respectively until DNA synthesis takes place or repair is completed.

Expression of the DNA integrity marker *PARP1* in galls suggests the induction of a DNA repair process activation in galls

Overall, our data support that nematodes may cause DNA damage during infection. In galls, high promoter activity in galls of the *PARP1* [poly(ADP-ribose) polymerase 2], a gene involved in the maintenance of DNA integrity during replication and the DNA repair process, has been observed (Lindahl *et al.*, 1995; de Murcia and de Murcia, 1994; Garcia *et al.*, 2003). *PARP1* expression throughout gall development is symptomatic of PARP1 function as an excision repair protein during the mitotic and endocycle phases going on in GCs. DNA repair might take place avoiding accumulation of GC nuclei with compromised genome impeding the proper feeding cell development. Expression in NCs suggest that these intensely dividing cells might sense DNA damage and activate the repair machinery giving cells the sufficient time to repair the damaged DNA before progressing into mitosis. As well, *PARP1* expression is under control of ATM/ATR thus suggesting their activation upon the hyper-activated mitotic activity in galls, when DNA damage occurs. ATM and ATR kinases not only activate DNA repair but also cell cycle checkpoint control driven by WEE1. As observed in plant cells, the nuclear PARP1 protein might bind to damaged DNA of gall cells and catalyze repair needed to ensure nuclear division. Higher *PARP1*expression in cells close to the nematode head suggests that nematode secreted proteins might cause DNA damage. Furthermore, we observed high *PARP1:GUS* (Babiychuk et al., 1998) activity in galls treated with BL and HU, known to induce the two Arabidopsis *PARP* genes in uninfected roots (Doucet-Chabeaud *et al.*, 2001; Chen *et al.*, 2003). Higher *PARP1* expression was seen upon HU and less upon BL treatment, similarly to what we observed for *WEE1*. Less PARP1 expression during BL treatment might be due to the inhibition of DNA-repair signaling or that nematode parasitism induces less double strand breaks. Our data suggest that the higher *WEE1* expression upon stress induced by HU in galls could be linked to checkpoint control activation followed by an induced DNA repair process marked by *PARP1* expression.

Tomato WEE1 downregulated line inhibited gall formation and nematode reproduction

Since the CDK inhibitory kinase WEE1 is involved in endoreduplication in tomato fruits (Gonzalez *et al.*, 2007), it is most likely that WEE1 has also a putative function at the DNA integrity checkpoints in

tomato. Indeed, SlWEE1 phosphorylates the mitotic CDK/CYCB complex, driving cells into the endocycle, thus contributing to cell enlargement and consequently to fruits of larger size (Gonzalez *et al.*, 2007). Besides keeping cells in a non-dividing state, SlWEE1 most likely operates during G1-to-S phase of the endocycle preventing a premature entry into the S phase of the following cycle (Gonzalez *et al.*, 2004; 2007). Nuclear DNA amplification according to the endoreduplication process may protect the genome from DNA-damaging conditions or prevent incorrect chromosome segregation during mitosis (Gonzalez *et al.*, 2007). As well upon damage, cell expansion induced by endoeduplication may compensate a decrease of cell number to keep tissue growth. Therefore, the function of SlWEE1 in the control of cell size and endoreduplication goes along with a putative function at the DNA integrity checkpoints. DNA amplification may require a sustained WEE1 activity to manage DNA damage potentially occurring during the intense DNA replication. Hence, we aimed at investigating the effects of a downregulation of SlWEE1 in nematode-induced tomato-galls. Similar to what occurs in tomato fruits, the downregulation of SlWEE1 in galls repressed the endocycle, and thus mitosis was induced, resulting in small galls alike decreased fruit size, both as results of decreased cell size. As in tomato fruits, the CDK/CYC Histone H1 kinase activity most likely increases upon WEE1 deficiency in galls.

DNA damage in hosts can be caused by nematodes and other pathogens

Living organisms encounter many types of DNA damage, therefore have evolved multiple mechanisms to maintain their genomic integrity. The present study hints that RKN induce DNA damage in plant hosts which might lead to chromosomal aberrations as formerly described by Starr (1993). This observation matches with the intricate nuclei morphology typically observed in GCs, even when the DNA repair machinery seems to be activated in galls (Antonino de Souza Junior et al., 2017). It is also recognized that microbial plant pathogens with diverse life styles, like hemibiotrophic bacterial species, oomycetes and necrotrophic fungi can induce DNA damage in the host plant genomes (Song and Bent, 2014). Interestingly, reduced levels of DNA DSBs may be observed during incompatible interactions when compared with compatible. Some pathogens are even able to use strategies to inactivate the DDR and circumvent the DNA damage checkpoints (Guerra *et al.,* 2011). So far, not much is known if pathogen-induced stress and DNA damage have preferential sites, but candidate compounds are effectors, toxins, or other molecules as reported for bacteria (Guerra *et al*., 2011). In addition, a link of DDR and the plant immune system like activation by salicylic acid (SA) and prevention of DNA repair in the host seem to occur, and similar links have been described for animal and human

pathogens (Song and Bent, 2014; Menendez *et al.,* 2011; Gasser *et al.,* 2005;). Thus, it will be interesting to address these questions during future studies.

Concluding remarks

Summing up, our data substantiate the hypothesis that the WEE1 kinase is involved in DNA damage and more notably in DNA replication checkpoint in galls induced by RKN. We here propose that stress caused by DNA damage threatens NFS formation, and hence that WEE1 activation helps the optimal NFS development during the coordinated events taking place in its hyperactivated cell cycle. Repair pathways in galls will most likely recognize to a certain level and restore a range of DNA anomalies, like mismatches, abnormal bases, stalled replication forks, single-stranded DNA nicks, and double-stranded DNA breaks (DSBs) (Friedberg *et al.*, 2006; Weitzman & Weitzman, 2014). Thus, nematodes seem not to circumvent checkpoint controls and manipulate the host DNA damage pathways as seen for some human microbes (Weitzman & Weitzman, 2014). As for uninfected roots, in galls the CDKA;1/CYCB complex might be the major target for inhibition by the activated checkpoint control through WEE1 kinase activity. In figure 14 we illustrate the involvement of WEE1 in the potential DNA damage occurring in nematode-induced galls and upon drug induced ectopic stress. It is possible that nematode derived effectors, toxins, or other molecules are be required for induction of DNA damage, and upcoming research will pinpoint if DNA damage is targeted to preferential sites. Thus, investigation of nematode factors or induced plant factors related to infection associated DNA damage may help us to envision nematode-induced disease management strategies that can protect the host against these plant pathogens.

Acknowledgments

We thank J. Cazareth for technical assistance for the flow cytometry analysis, N. Marteau for supplying us with pre-parasitic nematodes, H. Ballesteros for preparing the confocal images of *wee-1-1* inhibitor treatments with a CAPES-COFECUB Sv.622/18 grant. M. A. Figueroa with an Erasmus Mundus grant for help with analyses of *wee1-1* line; J. D. Antonino for a CAPES-COFECUB Sv683/10 grant, N. Rodiuc and R.R. Coelho for CSF-CNPq grants. DC is supported by CAPES-doctoral grant (99999.002114/2015-01).

Author Contributions

Conceived and designed the experiments: JdAE, DC, LDV. Performed the experiments: DC, MYB, JdAE, JDA, NR, GE, PV, RRC, TE. Analyzed the data: JdAE, DC, JDA, CC. Contributed

reagents/materials/analysis tools: LDV, CC, MFG-d-S. Wrote the paper: JdAE, DC. Amended the paper: JdAE, DC, LDV, CC, JDA.

References

1. **Aarts M, Linardopoulos S & Turner NC. 2013.** Tumour selective targeting of cell cycle kinases for cancer treatment. *Current Opinion in Pharmacology*, 13: 529-535.
2. **Adachi S, Minamisawa K, Okushima Y, Inagaki S, Yoshiyama K, Kondou Y, Kaminuma E, Kawashima M, Today T, Matsui M, Kurihara D, Matsunaga S & Kurihara, D. 2011.** Programmed induction of endoreduplication by DNA double-strand breaks in Arabidopsis. *Proceedings of the National Academy of Sciences*, *108*: 10004-10009.
3. **Antonino de Souza Junior JD, Pierre O, Coelho RR, Grossi-de-Sa MF, Engler G, & de Almeida Engler J. 2017.** Application of nuclear volume measurements to comprehend the cell cycle in root-knot nematode-induced giant cells. *Frontiers in Plant Science*, 8: 961.
4. **Babiychuk E, Cottrill PB, Storozhenko S, Fuangthong M, Chen Y, O'Farrell MK, Van Montagu M, Inzé D & Kushnir S. 1998**. Higher plants possess two structurally different poly (ADP-ribose) polymerases. *The Plant Journal*, 15: 635-645.
5. **Bergervoet JHW, Verhoeven HA, Gilissen LJW & Bino RJ. 1996.** High amounts of nuclear DNA in tomato (*Lycopersicon esculentum* Mill.) pericarp. *Plant Science*. 116: 141–145.
6. **Chen IP, Haehnel U, Altschmied L, Schubert I and Puchta H. 2003.** The transcriptional response of Arabidopsis to genotoxic stress – a high-density colony array study (HDCA). *The Plant Journal* 35: 771–786.
7. **Chevalier C, Nafati M, Mathieu-Rivet E, Bourdon M, Frangne N, Cheniclet C, Renaudin JP, Gévaudant F & Hernould M. 2011.** Elucidating the functional role of endoreduplication in tomato fruit development. *Annals of Botany*, 107: 1159-1169.
8. **Cools T, and De Veylder, L. 2009.** DNA stress checkpoint control and plant development. *Current Opinion in Plant Biology*. 12: 23–28.
9. **Cools T, Iantcheva A, Weimer AK, Boens S, Takahashi N, Maes S, Van de Daele H, Van Iserdael G, Schnittger A & De Veylder L. 2011.** The *Arabidopsis thaliana* checkpoint kinase WEE1 protects against premature vascular differentiation during replication stress. *The Plant Cell*, 23:1435-1448

10. **Culligan, K, Tissier A & Britt A. 2004.** ATR regulates a G2-phase cell-cycle checkpoint in Arabidopsis thaliana. *The Plant Cell* 16: 1091–1104.
11. **de Almeida Engler J, De Veylder L, De Groodt R, Rombauts S, Boudolf V, De Meyer B, Hemerly A, Ferreira P, Beeckman T, Karimi M, Hilson P, Inzé D & Engler G. 2009.** Systematic analysis of cell cycle gene expression during Arabidopsis development. *The Plant Journal*. 59: 645-660.
12. **de Almeida Engler J, De Vleesschauwer V, Burssens S, Celenza JLJr, Inzé D, Van Montagu M, Engler G & Gheysen G. 1999.** Molecular markers and cell cycle inhibitors show the importance of cell cycle progression in nematode-induced galls and syncytia. *The Plant Cell*, 11: 793-807.
13. **de Almeida Engler J, Kyndt T, Vieira P, Van Cappelle E, Boudolf V, Sanchez V, Escobar C, De Veylder L, Engler G, Abad P, & Gheysen G. 2012.** *CCS52* and *DEL1* genes are key components of the endocycle in nematode-induced feeding sites. *The Plant Journal*, 72: 185-198.
14. **de Almeida Engler J, Van Poucke K, Karimi M, De Groodt R, Gheysen G, Engler G & Gheysen G. 2004.** Dynamic cytoskeleton rearrangements in giant cells and syncytia of nematode infected roots. *The Plant Journal* 38: 12-26.
15. **de Almeida-Engler J, Siqueira KMS, Nascimento DC, Costa TG & Engler G. 2016.** A cellular outlook of galls induced by root-knot nematodes in the model host *Arabidopsis thaliana*. *Nematoda*, *1*: e062016.
16. **de Almeida-Engler J, Vieira P, Rodiuc N, Grossi-de-sa MF & Engler G. 2015.** The plant cell cycle machinery: usurped and modulated by plant parasitic nematodes. ***Advances in Botanical Research-Plant nematodes interactions***. The Plant Cell Cycle Machinery: Usurped and Modulated by Plant-Parasitic Nematodes. In C. Escobar & C. Fenoll (Eds.), *Plant Nematode Interactions: A View on Compatible Interrelationships.* Academic Press (pp. 91–118). ISBN: 9780124171619.
17. **de Murcia, G., & de Murcia, J. M. 1994.** Poly (ADP-ribose) polymerase: a molecular nick-sensor. *Trends in Biochemical Sciences*, 19: 172-176.
18. **De Schutter K, Joubès J, Cools T, Verkest A, Corellou F, Babiychuk E, Van Der Schueren, E, Beeckman T, Kushnir S, Inzé D & De Veylder L. 2007.** Arabidopsis WEE1 kinase controls cell cycle arrest in response to activation of the DNA integrity checkpoint. *The Plant Cell*, 19: 211-225.

19. **Do K, Doroshow JH & Kummar S. 2013**. Wee1 kinase as a target for cancer therapy. *Cell cycle*, 12: 3348-3353.
20. **Doucet-Chabeaud G, Godon C, Brutesco C, de Murcia G and Kazmaier M. 2001.** Ionising radiation induces the expression of PARP-1 and PARP-2 genes in Arabidopsis. *Molecular Genetics and Genomics*, 265: 954–963.
21. **Francis D. 2007.** The plant cell cycle− 15 years on. *New Phytologist*, 174: 261-278.
22. **Friedberg EC, Walker GC, Siede W, Wood RD, Schultz RA, Ellenberger T. 2006.** DNA Repair and Mutagenesis. Second Edition. New York: ASM Press.
23. **Gandarillas A, Molinuevo R, & Sanz-Gómez N. 2018.** Mammalian endoreplication emerges to reveal a potential developmental timer. *Cell Death & Differentiation* 25: 471-476.
24. **Garcia V, Bruchet H, Camescasse D, Granier F, Bouchez D & Tissier A. 2003.** *AtATM* is essential for meiosis and the somatic response to DNA damage in plants. *The Plant Cell* 15: 119–132.
25. **Gasser S, Orsulic S, Brown EJ, Raulet DH. 2005.** The DNA damage pathway regulates innate immune system ligands of the NKG2D receptor. *Nature* 436: 1186–1190.
26. **Gonzalez N, Gévaudant F, Hernould M, Chevalier C & Mouras A. 2007.** The cell cycle-associated protein kinase WEE1 regulates cell size in relation to endoreduplication in developing tomato fruit. *The Plant Journal*, 51: 642-655.
27. **Gonzalez N, Hernould M, Delmas F, Gévaudant F, Duffe P, Causse M, Mouras A & Chevalier C. 2004.** Molecular characterization of a WEE1 gene homologue in tomato (*Lycopersicon esculentum* Mill.). *Plant Molecular Biology*, 56: 849-861.
28. **Guerra L, Guidi R, Frisan T. 2011.** Do bacterial genotoxins contribute to chronic inflammation, genomic instability and tumor progression? *The FEBS Journal*; 278: 4577–4588.
29. **Halazonetis TD, Gorgoulis VG, Bartek J. 2008.** An oncogene-induced DNA damage model for cancer development. *Science* 319: 1352–5.
30. **Heyman J, & De Veylder L. 2012.** The anaphase-promoting complex/cyclosome in control of plant development. *Molecular Plant*, 5: 1182-1194.
31. **Hu Z, Cools T & De Veylder L. 2016.** Mechanisms used by plants to cope with DNA damage. *Annual review of plant biology*, 67: 439-462.
32. **Inzé D, De Veylder L. 2006.** Cell cycle regulation in plant development. *Annual Review in Genetics* 40: 77–105.

33. **Joubès, J, Phan TH, Just D, Rothan C, Bergounioux C, Raymond P & Chevalier C. 1999.** Molecular and biochemical characterization of the involvement of cyclin-dependent kinase CDKA during the early development of tomato fruit. *Plant Physiology* 121: 857–869.
34. **Lindahl T, Satoh MS, Poirier GG, & Klungland A. 1995.** Post-translational modification of poly (ADP-ribose) polymerase induced by DNA strand breaks. *Trends in Biochemical Sciences*, 20: 405-411.
35. **Mathieu-Rivet E, Gévaudant F, Cheniclet C, Hernould M, & Chevalier C. 2010.** The anaphase promoting complex activator CCS52A, a key factor for fruit growth and endoreduplication in tomato. *Plant Signaling & Behavior*, 5: 985-987.
36. **Menendez D, Shatz M, Azzam K, Garantziotis S, Fessler MB, et al. 2011.** The Toll-like receptor gene family is integrated into human DNA damage and p53 networks. *PLoS Genetics* 7: e1001360.
37. **Morin RD, Mendez-Lago M, Mungall AJ, Goya R, Mungall KL, Corbett RD, Johnson NA, Severson TM, Chiu R, Field M, et al. 2011.** Frequent mutation of histone-modifying genes in non-Hodgkin lymphoma. *Nature* 476: 298-303.
38. **Rafiei G. 2012.** Studies on the role of WEE1 in the plant cell cycle. PhD thesis, School of Biosciences, Cardiff University, United Kingdom
39. **Rodiuc N, Vieira P, Banora MY, & de Almeida Engler J. 2014.** On the track of transfer cell formation by specialized plant-parasitic nematodes. *Frontiers in Plant Science*, 5: 160.
40. **Russell P & Nurse P. 1987.** Negative regulation of mitosis by wee1+, a gene encoding a protein kinase homolog. *Cell*, 49: 559-567.
41. **Saban N & Bujak M. 2009.** Hydroxyurea and hydroxamic acid derivatives as antitumor drugs. *Cancer Chemotherapy and Pharmacology* 64: 213–221.
42. **Shukla N, Yadav R, Kaur P, Rasmussen S, Goel S, Agarwal M, Jagannath A, Gupta R & Kumar A. 2018.** Transcriptome analysis of root-knot nematode (*Meloidogyne incognita*)-infected tomato (*Solanum lycopersicum*) roots reveals complex gene expression profiles and metabolic networks of both host and nematode during susceptible and resistance responses. *Molecular Plant Pathology*, 19: 615-633.
43. **Siciliano I., Grønlund AL., Ševčíková H., Spadafora ND., Rafiei G., Francis D., Herbert MRJ, Bitonti MB., Rogers HJ. & Lipavská, H. 2019.** Expression of Arabidopsis WEE1 in tobacco induces unexpected morphological and developmental changes. *Scientific Reports*, 9: 8695.

44. **Song J & Bent AF. 2014.** Microbial pathogens trigger host DNA double-strand breaks whose abundance is reduced by plant defense responses. *PLoS Pathogens,*10: e1004030.
45. **Sorrell DA, Marchbank A, McMahon K, Dickinson RJ, Rogers HJ & Francis D. 2002.** A WEE1 homologue from *Arabidopsis thaliana*. *Planta*, 215: 518-522.
46. **Spadafora ND, Doonan JH, Herbert RJ, Bitonti MB, Wallace E, Rogers HJ & Francis D. 2010.** Arabidopsis T-DNA insertional lines for CDC25 are hypersensitive to hydroxyurea but not to zeocin or salt stress. *Annals of Botany*, 107: 1183-1192.
47. **Starr, J.L. 1993.** Dynamics of the nuclear complement of giant cells induced by *Meloidogyne incognita*. *Journal of Nematology*. **25,** 416–421.
48. **Sun Y, Dilkes BP, Zhang C, Dante RA, Carneiro NP, Lowe KS, Jung R, Gordon-Kamm WJ & Larkins BA. 1999.** Characterization of maize (*Zea mays L.*) Wee1 and its activity in developing endosperm. *Proceedings of the National Academy of Sciences*, 96: 4180-4185.
49. **Takimoto CH & Calvo E. 2008. "**Principles of Oncologic Pharmacotherapy." Ch 3 Appendix 3, in Pazdur R, Wagman LD, Camphausen KA, Hoskins WJ (Eds) Cancer Management: A Multidisciplinary Approach, 11th edition. Available: https://www.cancernetwork.com/articles/principles-oncologic-pharmacotherapy
50. **Van Leene, J, Hollunder, J, Eeckhout, D, Persiau G, Van De Slijke E, Stals, H., Van Isterdael G, Verkest A, Sandy Neirynck S, Buffel Y, et al. 2010.** Targeted interactomics reveals a complex core cell cycle machinery in *Arabidopsis thaliana*. *Molecular Systems Biology*, 6: 397.
51. **Vieira P, De Clercq A, Stals H, Van Leene J, Van De Slijke E, Van Isterdael G, Eeckhout D, Persiau G, Van Damme D, Verkest A, *et al.* 2014.** The cyclin-dependent kinase inhibitor KRP6 induces mitosis and impairs cytokinesis in giant cells induced by plant-parasitic nematodes in Arabidopsis. *The Plant Cell*, 26: 2633-2647. http://dx.doi.org/10.1105/tpc.114.126425.PMid:24963053.
52. **Vieira P, Engler G, & de Almeida Engler J. 2012.** Whole-mount confocal imaging of nuclei in giant feeding cells induced by root-knot nematodes in Arabidopsis. *New Phytologist*, 195: 488-496.
53. **Vieira P, Escudero C, Rodiuc N, Boruc J, Russinova E, Glab N, Mota M, De Veylder L, Abad P, Engler G & de Almeida Engler, J. 2013.** Ectopic expression of Kip-related proteins restrains root-knot nematode-feeding site expansion. *New Phytologist*, 199: 505-519.

54. **Vuolo F, Kierzkowski D, Runions A, Hajheidari M, Mentink RA, Gupta MD, Zhang** Z, **Vlad D, Wang Y, Pecinka A, et al. 2018.** LMI1 homeodomain protein regulates organ proportions by spatial modulation of endoreduplication. *Genes & Development*, 32: 1361-1366.
55. **Wang C & Liu Z. 2006.** Arabidopsis ribonucleotide reductases are critical for cell cycle progression, DNA damage repair, and plant development. *The Plant Cell* 18: 350–365.
56. **Wei Y, Mizzen CA, Cook RG, Gorovsky MA & Allis CD. 1998.** Phosphorylation of histone H3 at serine 10 is correlated with chromosome condensation during mitosis and meiosis in Tetrahymena. *Proceedings of the National Academy of Sciences*, 95: 7480-7484.
57. **Weitzman MD & Weitzman JB. 2014.** What's the damage? The impact of pathogens on pathways that maintain host genome integrity. *Cell Host & Microbe*, 15: 283-294.
58. **Yan S, Wang W, Marques J, Mohan R, Saleh A, Durrant W, Song J. & Dong Z. 2013.** Salicylic acid activates DNA damage responses to potentiate plant immunity. *Molecular Cell* 52: 602-610.73.
59. **Yi D, Alvim Kamei CL, Cools T, Vanderauwera S, Takahashi N, Okushima Y, Eekhout T, Yoshiyama KO, Larkin J, Van den Daele H, et al. 2014.** The *Arabidopsis* SIAMESE-RELATED cyclin-dependent kinase inhibitors SMR5 and SMR7 regulate the DNA damage checkpoint in response to reactive oxygen species. *The Plant Cell* **26**: 296–309.
60. **Yoshiyama, K., Sakaguchi, K., & Kimura, S. 2013.** DNA damage response in plants: conserved and variable response compared to animals. *Biology*, 2: 1338-1356.
61. **Zeman MK, Cimprich KA. 2014.** Causes and consequences of replication stress. *Nature Cell Biology* 16 :2–9

Legends

Fig. 1 Expression profile of *WEE1* varied during *Meloidogyne incognita*-induced gall development in Arabidopsis. **(a)** Dark-field micrographs illustrate *WEE1pro:GUS* staining (red) at different time points of gall development (3, 5, 7, 14, 21 and 30 DAI). **(b)** mRNA in situ localization of *WEE1* in galls 7, 14 and 21 DAI. Gall sections were hybridized with 35S-labeled antisense RNA probes. The hybridization signal is visible as white dots in dark-field optics. Giant cells are delineated with punctuated white lines. Days after inoculation, DAI; asterisk, giant cell; n, nematode. Bars, 50µm.

Fig. 2 WEE1 is nuclear localized in *Meloidogyne incognita*-induced Arabidopsis galls. Three-dimensional (3D) confocal microscopic projections of GFP-*WEE1* protein fusion (green)for *in vivo* visualization in whole galls. **(a, b, c)** Nematode-infected roots 3 and 5 DAI showing nuclear localization of GFP-WEE1 within two young feeding sites (FS1 and FS2). **(d, e)** Feeding sites 6 and 7 DAI showing more intense fluorescence of GFP-WEE1 in giant cells nuclei. Days after inoculation, DAI; FS1, feeding site 1; FS2, feeding site 2; Asterisk, giant cells; n, nematode. Bars = 100µm (a, b, c) and 50µm (d, e).

Fig 3. Morphological analysis of *Meloidogyne incognita*-induced galls in the *wee1-1* line of Arabidopsis showed induced mitotic activity compared to the wild-type. Bright-field images of longitudinal gall sections toluidine blue stained of **(a)** *wee1-1* galls 1, 3, 5, 7, 14 and 21 DAI and for **(b)** wild-type (Col-0) galls 3, 7, 14, 21 DAI. Black arrows point to cell wall stubs, red arrow to cell wall thickenings containing invaginations in giant cells, and white arrow points to multiple grouped nuclei (nu) of a *wee1-1* giant cell containing large number of nuclei. Ectopic neighboring cell and xylem division and relatively small giant cells are visible in *wee1-1* mature galls 21 DAI **(a)** compared to **(b)** wild-type. Days after inoculation, DAI; asterisk, giant cell; n, nematode; NCs, neighboring cells. Bars = 50µm.

Fig. 4 Altered nuclear morphology and volume is seen upon WEE1 knockout in *Meloidogyne incognita*-induced giant cells. Images illustrate 3D confocal projections of serial optical sections of thick gall slices stained with 4,6-diamidino-2-phenylindole (DAPI). **(a)** Galls in the *wee1-1* line 14 days after inoculation (DAI). Elongated nuclei apparently connected are observed in giant cells (orange arrows) suggesting accumulation of mitotic defects upon inhibition of the cell cycle checkpoint control activation in *wee1-1* galls. **(b)** Wild-type galls 14 DAI. Most nuclei are amoeboid shaped in wild-type giant cells. n, nematode; NCs, neighboring cells. Bars = 50 µm. (c) Nuclear volume of giant cells 14 DAI. The distribution is shown by the vertical box plots. The lines within the boxes indicate the median of nuclei volumes and the upper and lower box edge indicate variation of 25 to 75%. The bars show the largest/smaller values of average volumes that fall within a distance of 1.5 times IQR (interquartile range) from the upper and lower hinges, and the dots are the values that fall outside the IQR (outliers). The statistical difference is marked with asterisks ($P<0.001$) based on Student's t-test analysis.

Fig. 5 Flow cytometry examination of wild-type and *wee1-1* in *Meloidogyne incognita*-induced galls in Arabidopsis reveals a shift of root and gall cells into a mitotic state. **(a)**Percentage of nuclei with various ploidy levels in uninfected roots (2C to 16C) in wild-type plants compared with *wee1-1*. **(b)** Percentage of ploidy levels in galls 21 DAI (2C to 64C) in wild-type compared with *wee1-1*. Ploidy levels were statistically compared using Student's t-test, with * meaning P ≤0.05, ** P≤0.01 and n.s. not significative. Both uninfected roots and galls presented higher 2C ploidy levels suggesting increased mitotic activity upon lack of WEE1.

Fig. 6 Promoter activity of the **(a)** *SMR7:GUS* in the *wee1-1* knockout background and **(b)** *SMR7:GUS* in the wild-type of *Meloidogyne incognita*-induced galls. Dark-field images illustrate GUS staining in red in galls at 7, 14 and 21 days after inoculation (DAI). Note higher promoter activity in the transgenic line under the *wee1-1* background suggesting that lack of checkpoint control due the absence of WEE1 will induce a stress induced SMR7 promoter in developing galls. Days after inoculation, DAI; asterisk, giant cell; n, nematode. Bars = 50µm.

Fig. 7 Expression patterns of *Meloidogyne incognita*-induced galls in Arabidopsis WEE1pro:GUS line, and gall morphology of *wee1-1* line and wild-type (WT) Arabidopsis non-treated (NT), and bleomycin (+BL) or hydroxyurea (+HU) treatments. **(a)** Dark-field images illustrate GUS staining in red in galls 10). **(b)** Bright-field images of longitudinally sectioned galls 21 DAI stained with toluidine blue in the *wee1-1* knockout line NT, and BL and HU treated. **(c)** Bright-field images of longitudinally sectioned galls 21 DAI stained with toluidine blue in the WT NT, and BL and HU treated. Black arrows show wall stubs present in giant cells after BL and HU treatment. DAI, days after inoculation; asterisk, giant cell; n, nematode; NC, Neighboring cells. Bars = 50µm.

Fig. 8 3D projections of giant cell nuclear structure revealed changes in *WEE1* knockout and wild-type *Meloidogyne incognita*-induced galls in Arabidopsis **(a, d)** non-treated and **(b,c,e,f)** treated with the stress inducing drugs bleomycin (BL) or hydroxyurea (HU). All images are the result of projections of serial optical sections of galls 21 days after inoculation stained with 4,6-Diamidino-2-phenylindole (DAPI). Elongated nuclei were observed in the *wee1-1* knockout line and these became apparently unstructured and enlarged upon drug treatment. Bars = 50 µm.

Fig. 9 *Meloidogyne incognita*-induced giant cell area measurements and infection tests in the *wee1-1* knockout line and wild-type Arabidopsis non-treated (NT) and treated with stress inducing drugs bleomycin (BL) or hydroxyurea (HU). (a) Giant cell area measurements in galls non-treated and treated with BL or HU, and (b) gall and (c) egg mass number. Curiously BL and HU treatments of the *wee1-1* knockout line resulted in increased number of galls and egg masses. Analysis of variance (ANOVA) were done to compare treatments in the same line (WT or *wee1-1*), using Tukey test to compare means ($P<0.05$). To compare different lines in the same drug treatment we used pairwise comparisons using Student's t-test ($P<0.05$). Different capital letters mean statistical difference (ANOVA) between WT treatments, and small letters means difference in *wee-1* line treatments. * means $P\leq0.05$ and *** $P\leq0.001$

Fig. 10 Expression profile of *PARP1* in *Meloidogyne incognita*-induced galls in Arabidopsis non-treated and treated with the stress inducing drugs bleomycin (BL) and hydroxyurea (HU). Dark-field micrographs illustrate GUS in red. **(a)** *PARP1:GUS* staining (16 h of incubation with substrate) at different time points of gall development (7, 14 and 21 DAI). **(b)** *PARP1:GUS* staining (3h of incubation) in untreated galls 10 DAI and after stress inducing BL and HU treatments. Note that HU significantly induces *PARP1* promoter activity in galls. Note that giant cells close to the nematode head show higher GUS activity. Days after inoculation, DAI; asterisk, giant cell; n, nematode. Bars = 50µm.

Fig. 11 Morphological analysis of *Meloidogyne incognita*-induced galls in wild-type (WT) and *WEE1*^{AS} lines of tomato (*Solanum lycopersicum*). Giant cells in **(a)** wild-type are visibly larger compared to the **(b)** *WEE1*^{AS} line and nematodes are delayed in their development. Days after inoculation, DAI; asterisk, giant cell; n, nematode. Bars = 100 µm.

Fig. 12 Nuclei in *Meloidogyne incognita*-induced tomato galls of **(a)** wild-type (WT) and **(b)** *WEE1*^{AS} line. Fluorescent nuclei are 4,6-diamidino-2-phenylindole (DAPI) stained in galls 7, 14, 30 DAI. Note multiple small nuclei in giant cells seen in the *WEE1*^{AS} line compared to wild-type. Days after inoculation, DAI; asterisk, giant cells; n, nematode; G, gall. Numbers after 'G' or 'n' is for differentiate galls or nematodes, respectively, in a same image. Bars = 100µm.

Fig. 13 *Meloidogyne incognita*-induced tomato giant cell area **(a)** and nematode infection tests **(b)** of the *WEE1*^{AS} line in tomato plants compared to wild-type (WT). Giant cells were significantly smaller as well as the number of egg-masses decreased in nematode infected roots of *WEE1*^{AS} transgenic lines. Pairwise comparisons were made using Student's t-test with * meaning P≤0.05 and ** P≤0.01.

Fig. 14 An overview for the WEE1 kinase function in galls induced by root-knot nematodes (*Meloidogyne incognita*) is presented. (a) In normal conditions (wild-type galls), nematode infection in the plant host will likely induce single strands breaks (SSBs) and to less extend double strand breaks (DSBs) (low *SMR7* promoter activity) leading to WEE1 expression. This implies checkpoint control activation in galls, resulting on cell cycle delay/arrest most likely during G1/S phase. Successively, DNA is restored once DNA repair pathway is recruited (*PARP1* promoter activity). Then, cell cycle progresses in galls leading to susceptibility of the plant host. (b) Nematode infection in the model host Arabidopsis on the absence of WEE1 (-WEE1) will lead to DNA damage marked by the hyper-activation of the stress marker *SMR7* promoter. No WEE1 induced checkpoint control activation, cell cycle progresses in galls inducing premature entry in mitosis resulting in cumulative mitotic defects. The observed phenotype will result in decreased giant cells and gall size and consequently negatively affecting nematode susceptibility. (c) Upon induced DNA damage in wild-type galls, SSBs caused by hydroxyurea (HU) and DSBs caused by bleomycin (BL) activates *WEE1* expression most likely inducing a replication arrest checkpoint at G1/S (high *WEE1* expression) and to a less extend G2/M (low *WEE1* expression). This will lead to a delay/arrest in the cell cycle followed by the activation of DNA repair marked by PARP1 expression, finally inhibiting mitotic activity in galls and leading to a significant decrease in nematode susceptibility. (d) Similar drug treatments in *wee1-1* galls induced DNA damage in galls causing SSBs triggered by HU and DSBs caused by BL. The absence of WEE1 likely prevented checkpoint control activation in galls resulting in premature mitosis, which upon ectopic stress caused by both drugs (HU and BL) surprisingly promoted increased nematode susceptibility.

Supporting Information

Fig. S1 Histograms illustrating flow cytometry analysis of Arabidopsis *wee1-1 Meloidogyne incognita*-induced galls and uninfected roots.

Fig. S2 Detailed expression profile of *WEE1* in *Meloidogyne incognita*-induced galls treated with hydroxyurea.

Fig. S3. Nuclei in *A. thaliana wee1-1* knockout and wild-type *Meloidogyne incognita*-induced galls.

Fig. S4 Morphological analysis of *Meloidogyne incognita*-induced galls in the *WEE1^{AS}* tomato line.

Fig. S5 Flow Cytometry analysis in tomato root and *Meloidogyne incognita*-induced galls in wild-type and *WEE1^{AS}* lines.

Video S1 3D confocal projections of serial optical sections of a 21-d-old gall induced by *M. incognita* in Arabidopsis *wee1-1* roots.

Video S2 3D confocal projections of serial optical sections of a 21-d-old gall induced by *M. incognita* in Arabidopsis *wee1-1* roots treated with bleomycin.

Video S3 3D confocal projections of serial optical sections of a 21-d-old gall induced by *M. incognita* in Arabidopsis *wee1-1* roots treated with hydroxyurea.

Video S4 3D confocal projections of serial optical sections of a 21-d-old gall induced by *M. incognita* in Arabidopsis wild-type roots.

Video S5 3D confocal projections of serial optical sections of a 21-d-old gall induced by *M. incognita* in Arabidopsis wild-type roots treated with bleomycin.

Video S6 3D confocal projections of serial optical sections of a 21-d-old gall induced by *M. incognita* in Arabidopsis wild-type roots treated with hydroxyurea.

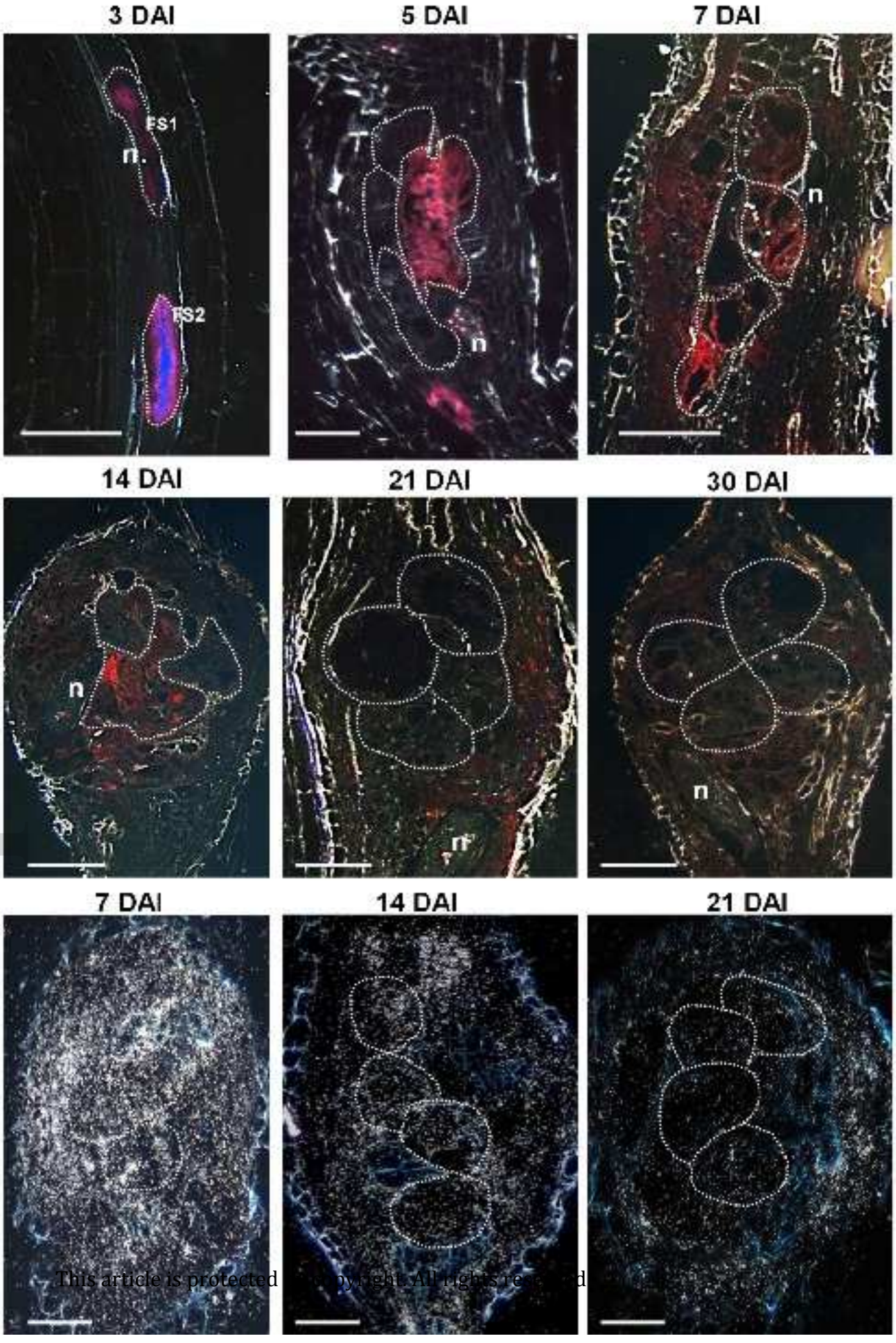

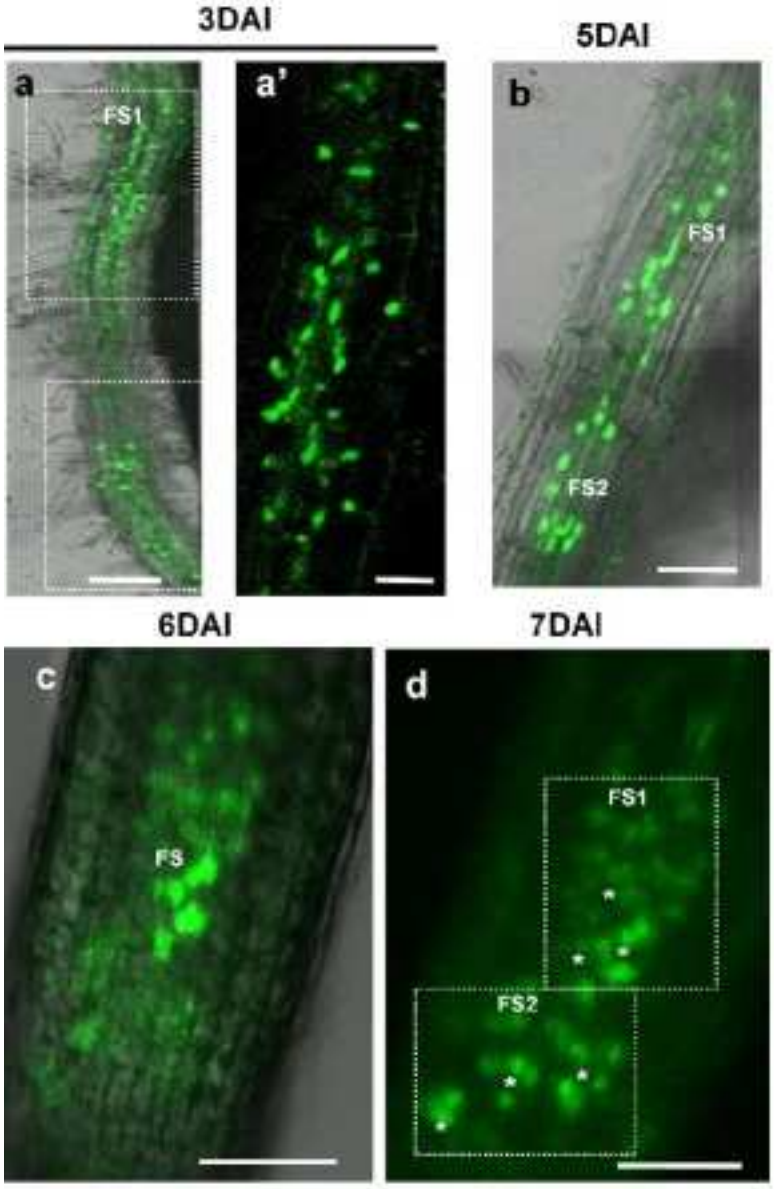

nph_16185_f2.tif

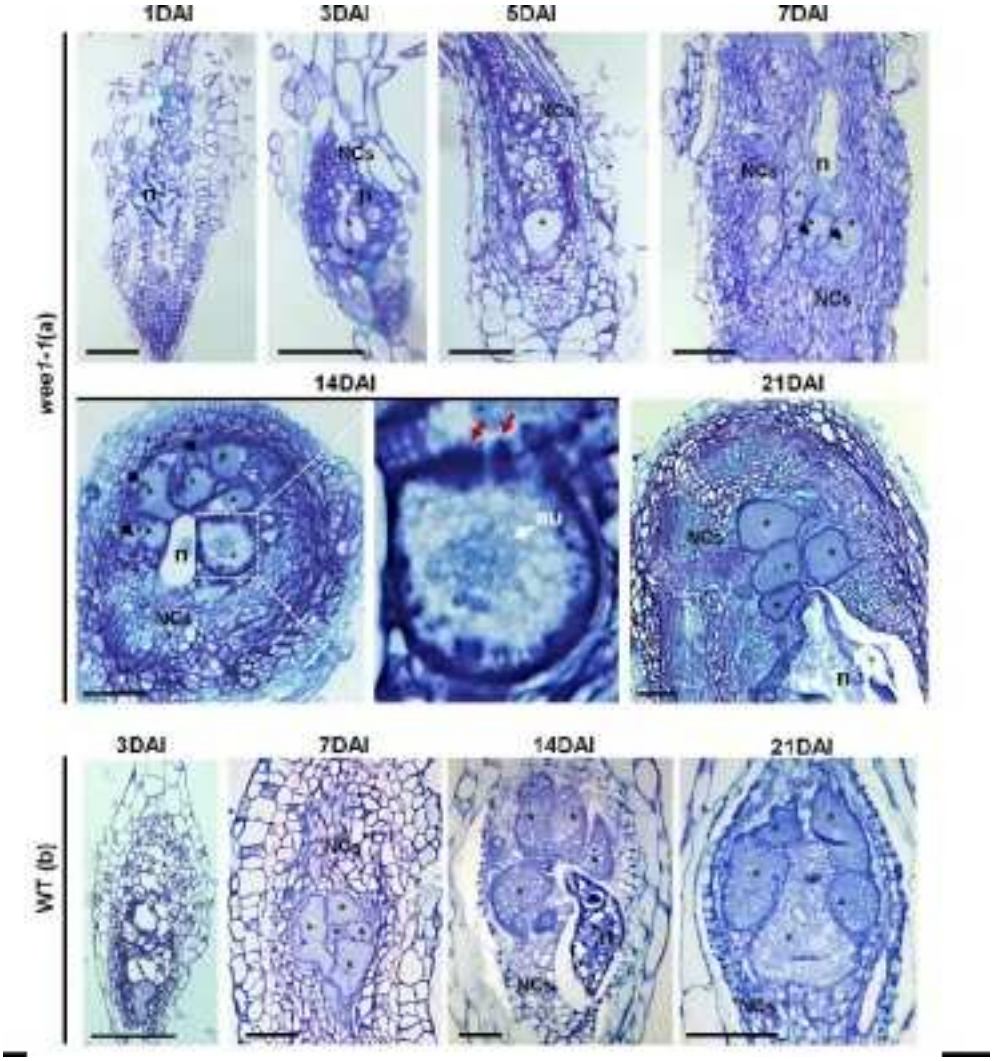

nph_16185_f3.tif

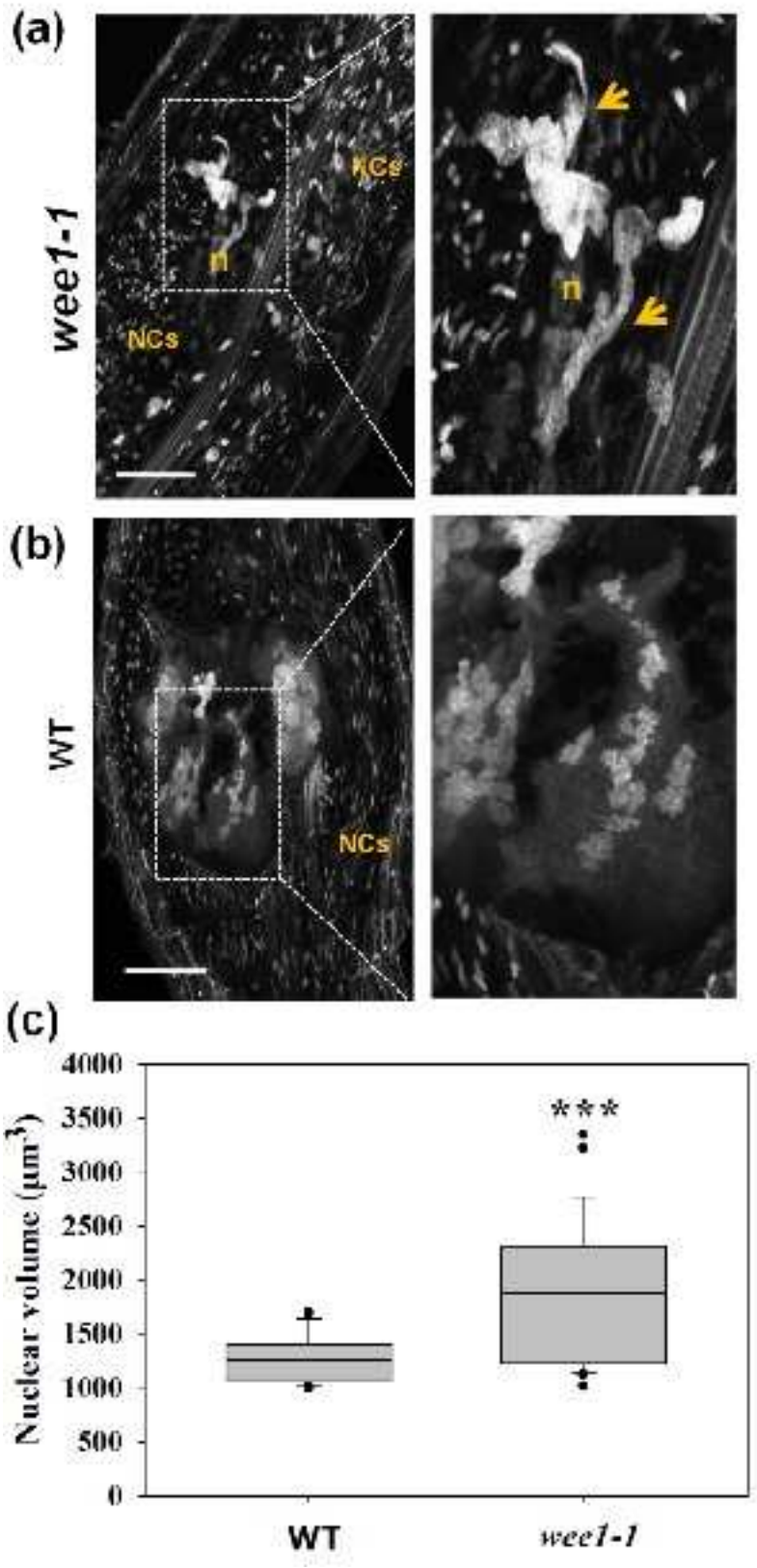

nph_16185_f4.tif

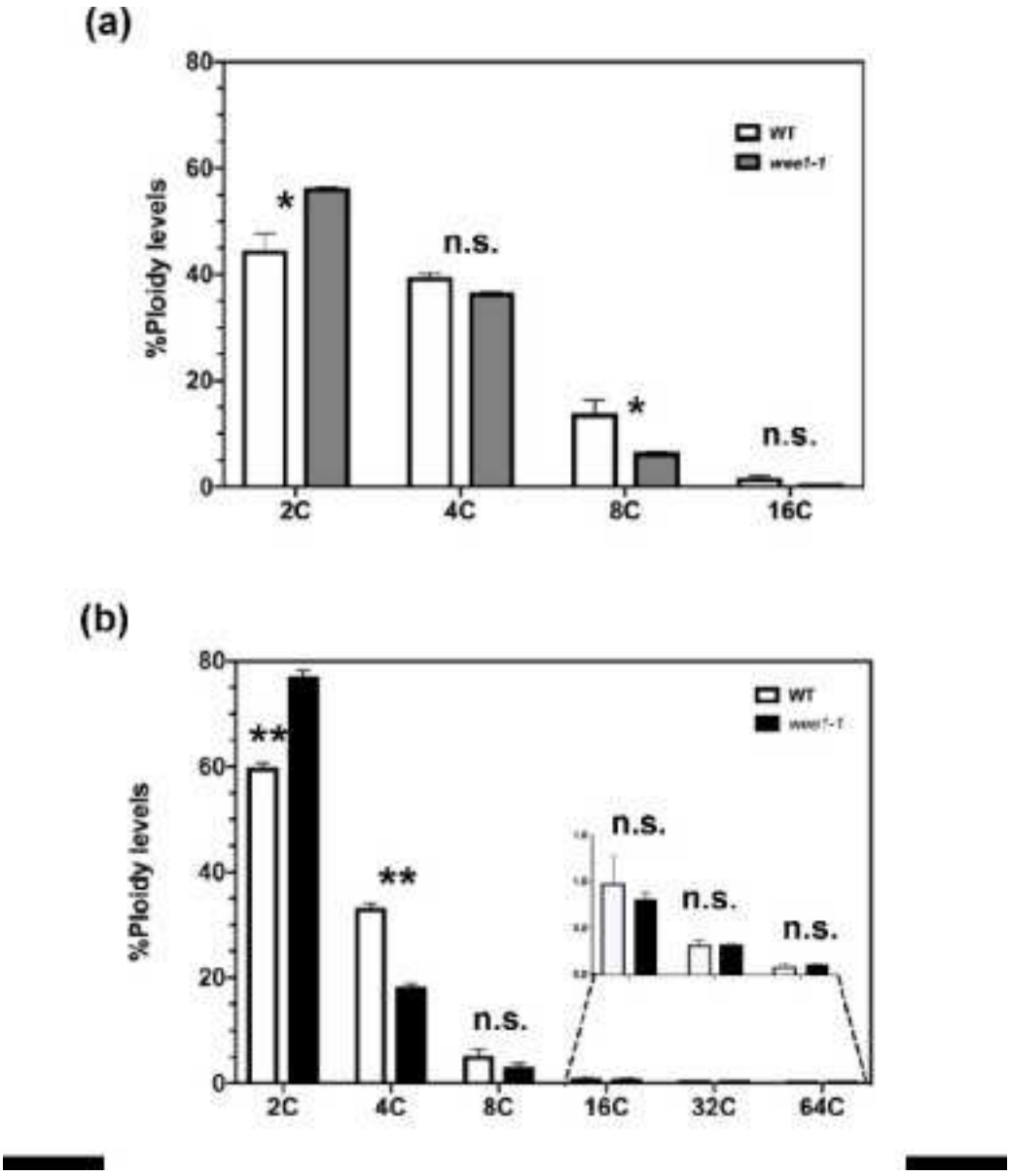

nph_16185_f5.tif

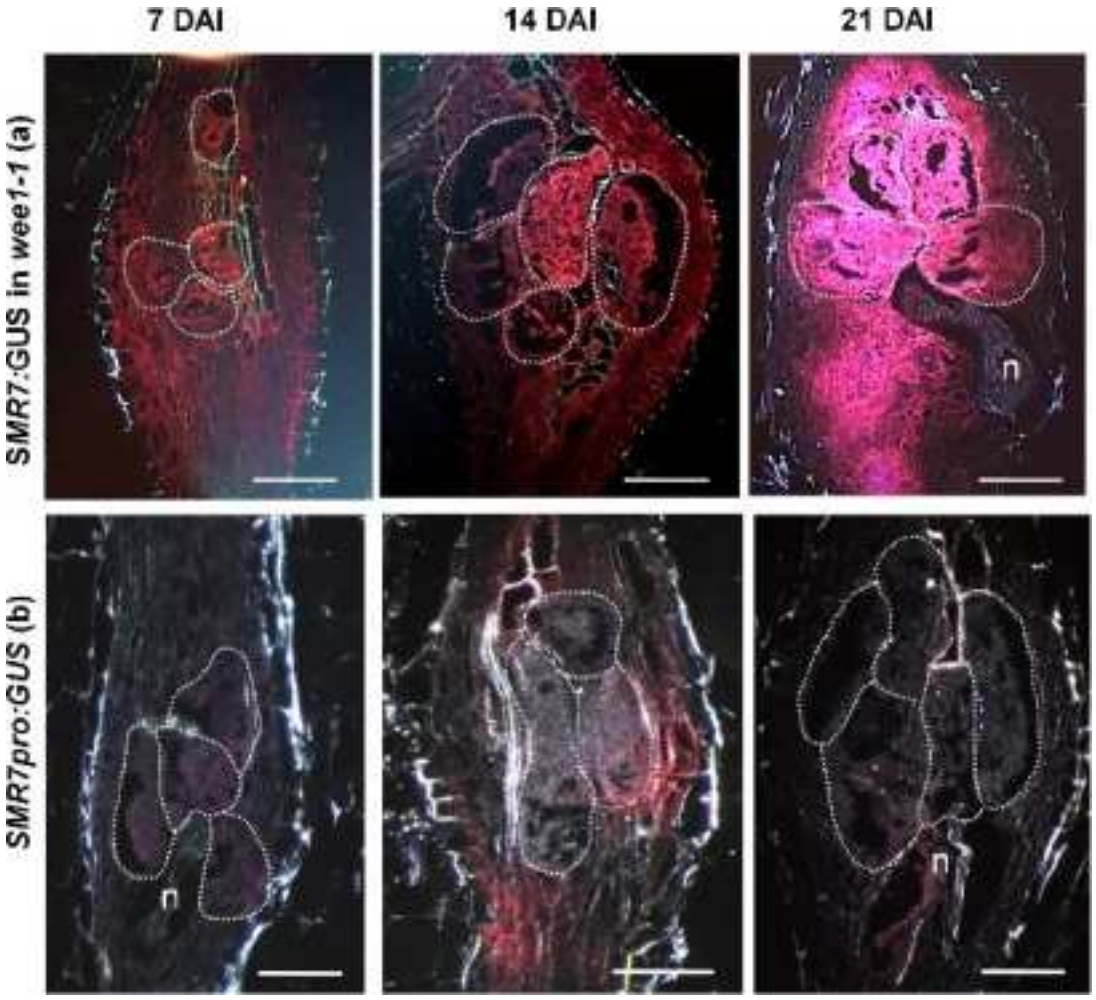

nph_16185_f6.tif

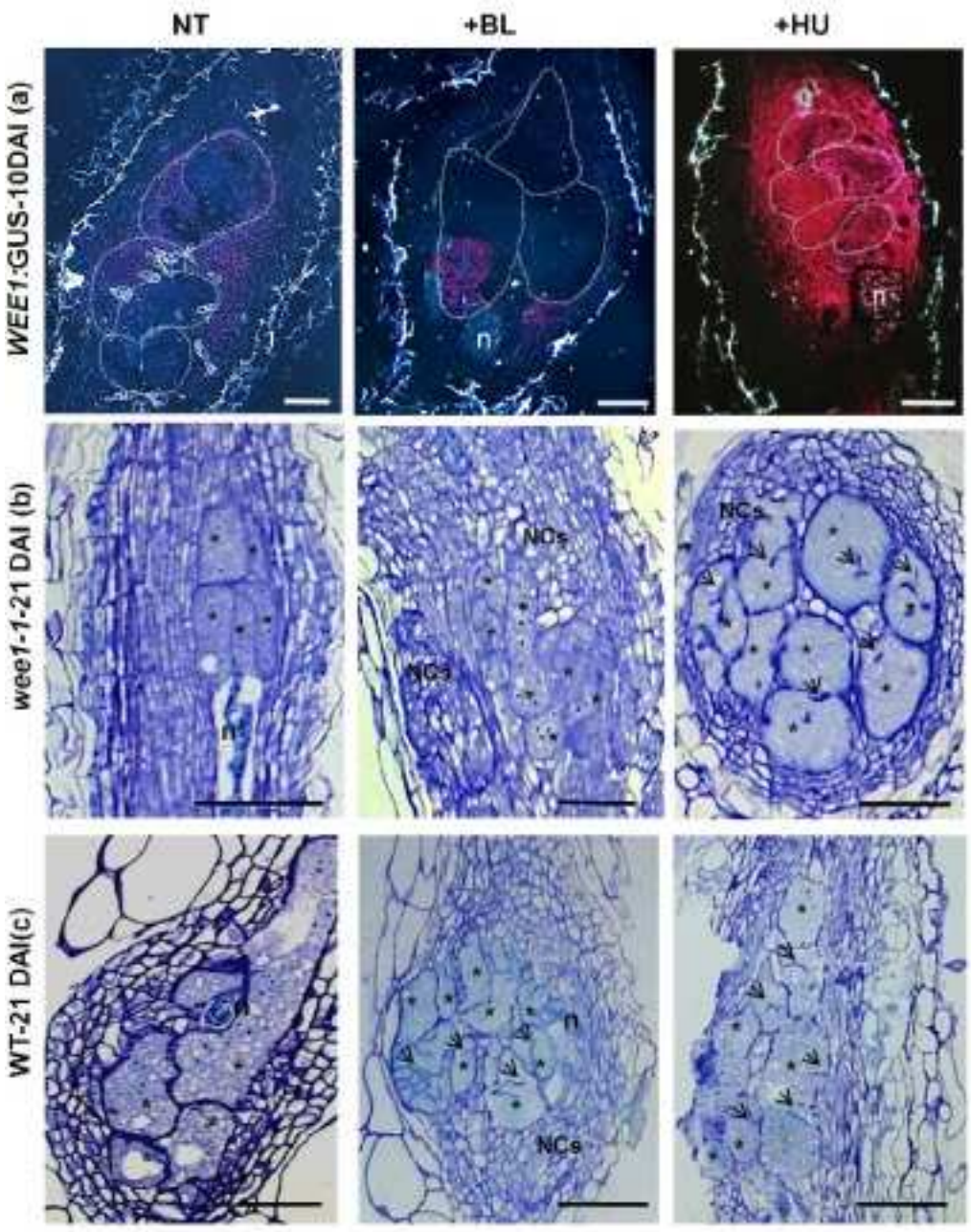

nph_16185_f7.tif

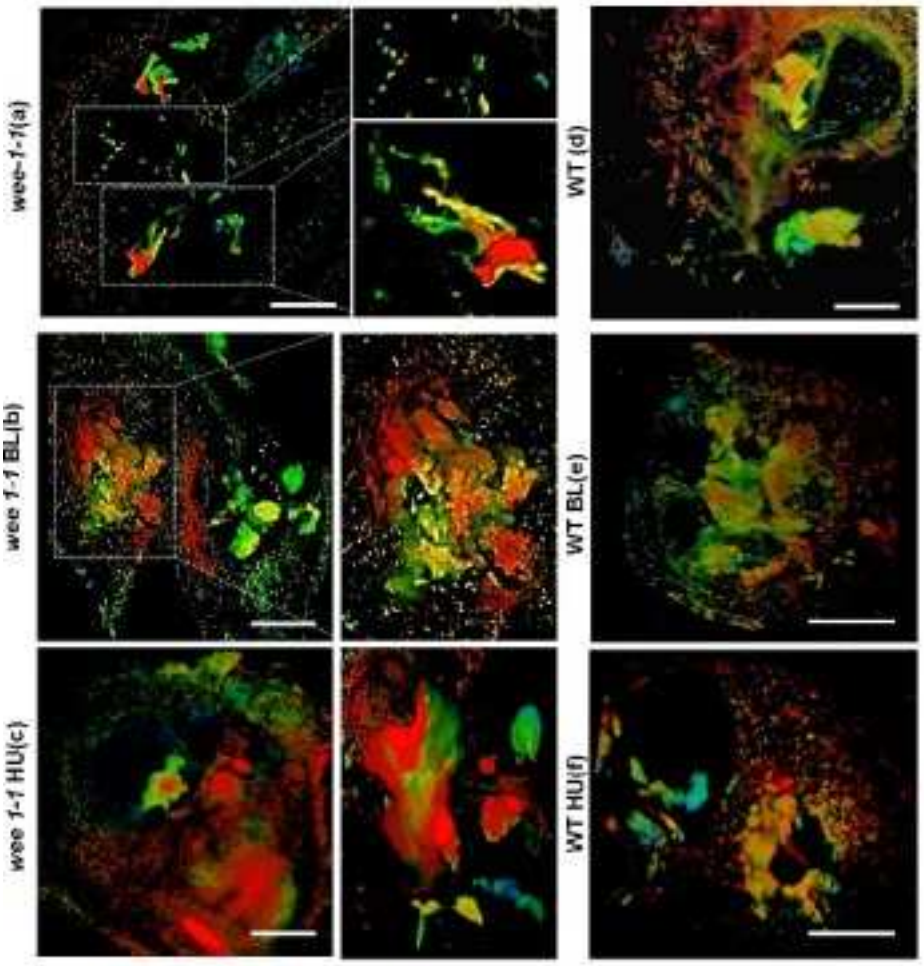

nph_16185_f8.tif

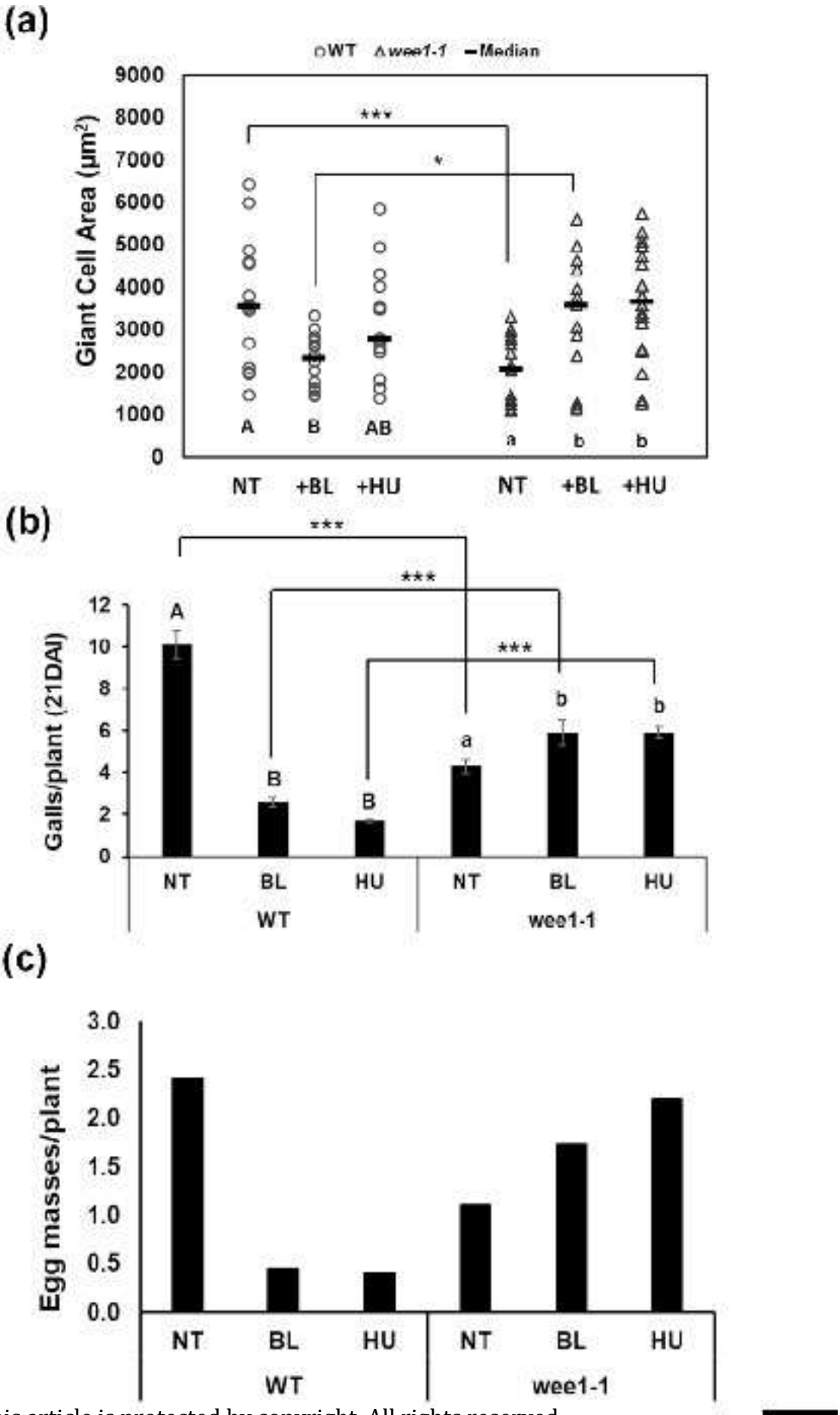

nph_16185_f9.tif

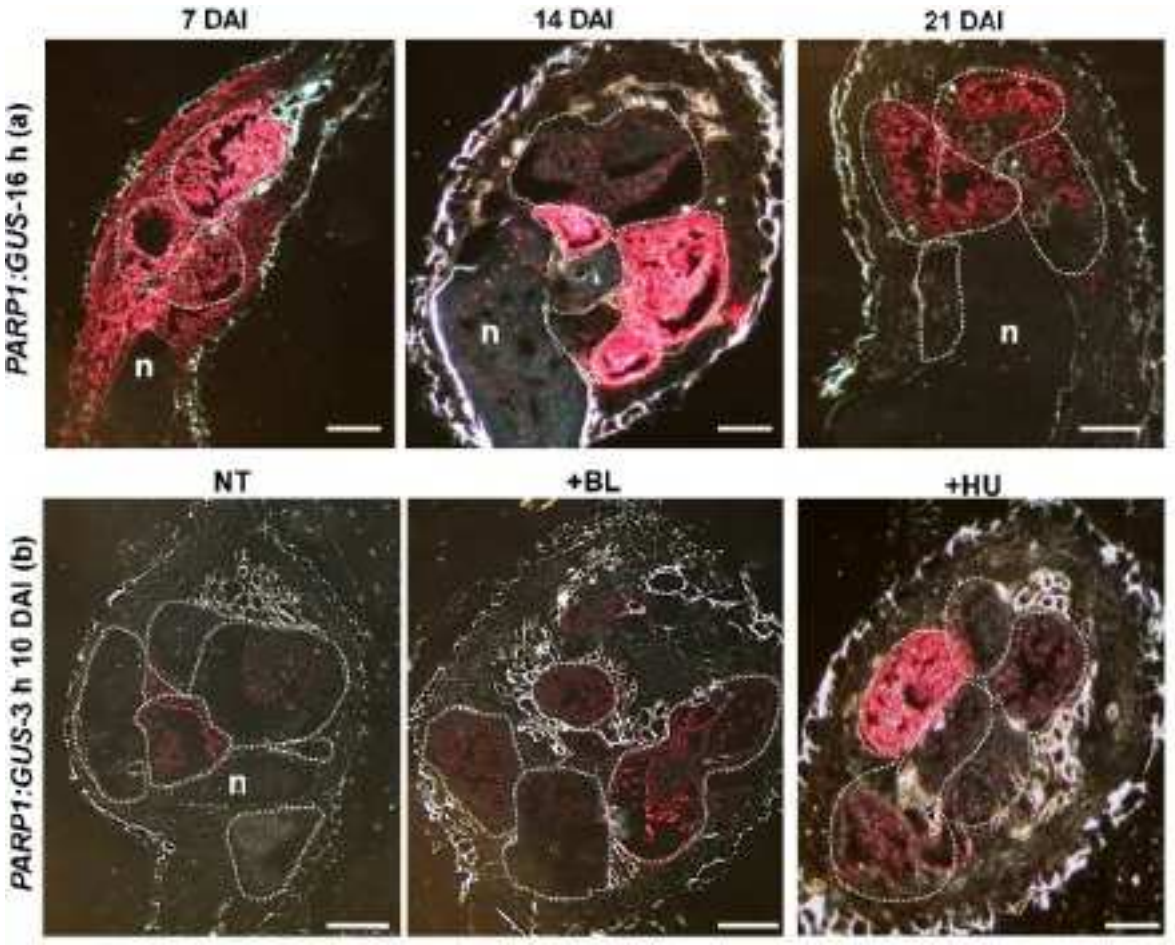

nph_16185_f10.tif

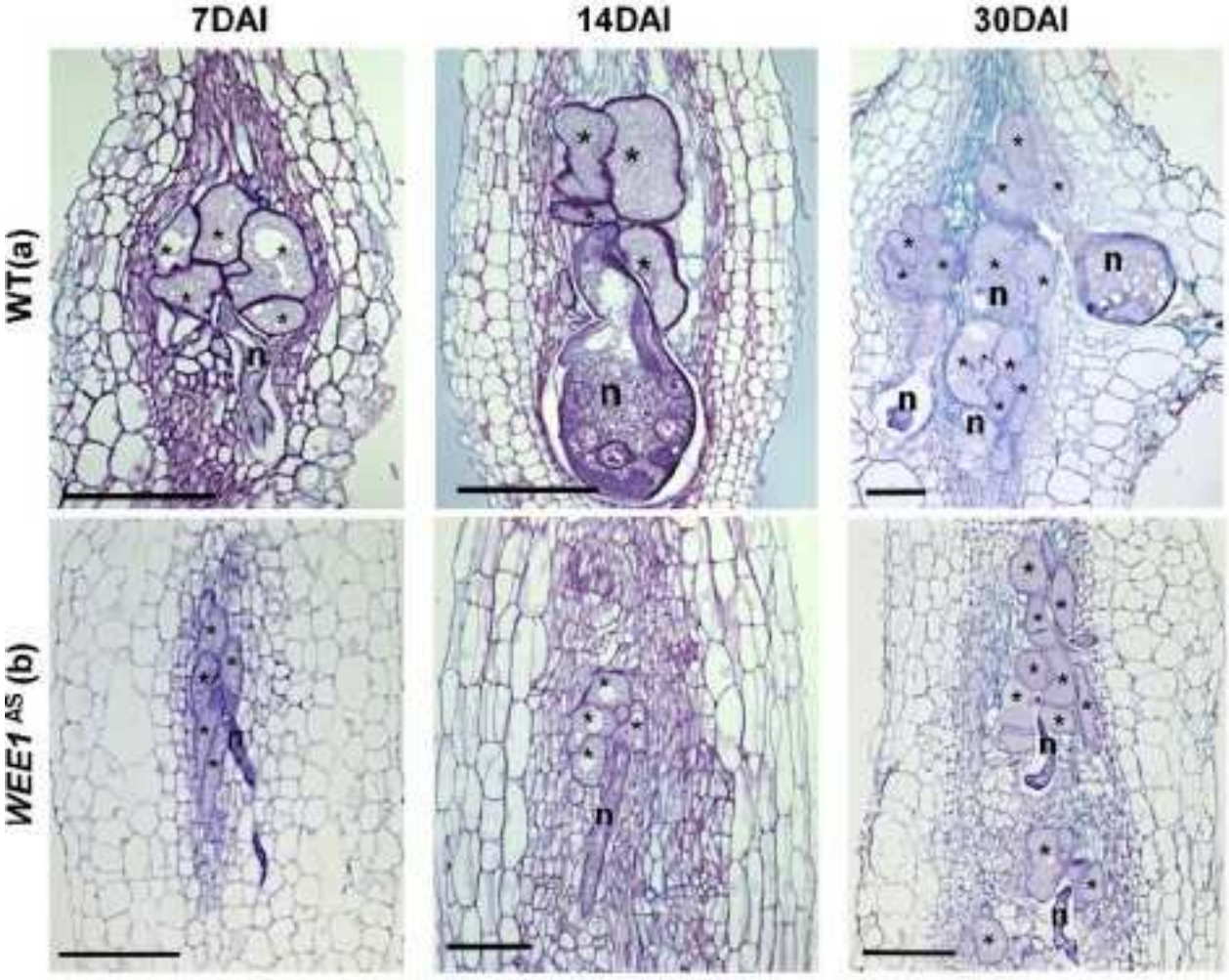

nph_16185_f11.tif

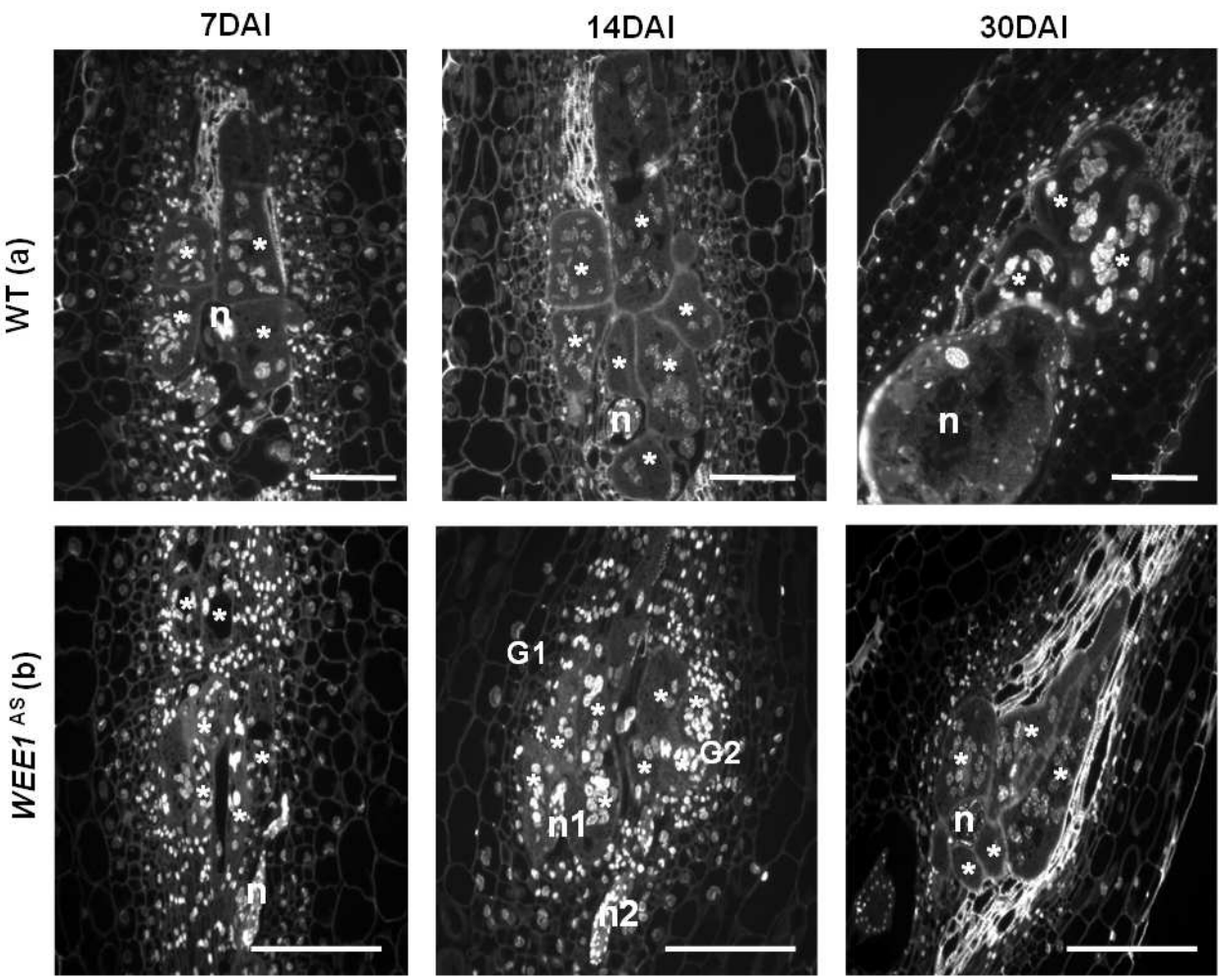

nph_16185_f12.tif

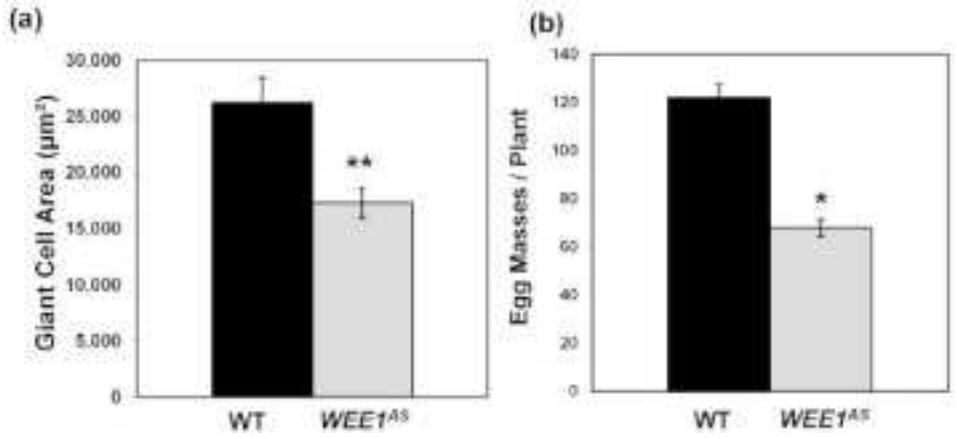

nph_16185_f13.tif

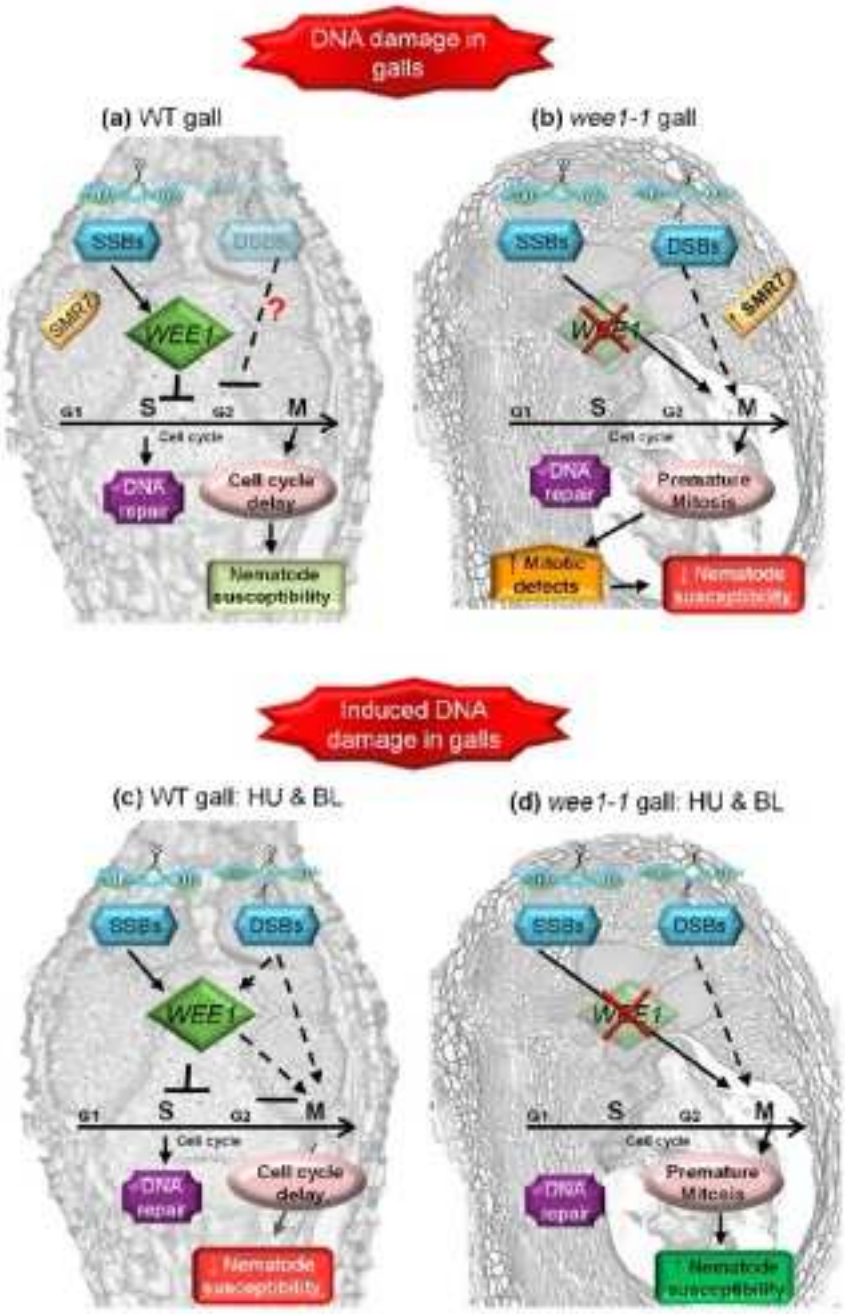

nph_16185_f14.tif